Exploiting Interactions of Multiple Interference for Cooperative Interference Alignment

Zhao Li, *Member, IEEE*, Jun Li, Yinghou Liu, Xiujuan Liang, Kang G. Shin, *Life Fellow, IEEE*, Zheng Yan, *Senior Member, IEEE*, and Hui Li, *Member, IEEE*

***Abstract*— Wireless networks are usually deployed to cover more overlapping areas, experiencing severe interferences and hence making interference management essential for their viability. Interference alignment (IA) is an effective way of interference management and has thus received significant attention. With IA, at least one degree-of-freedom (DoF) should be used to place the aligned interferences. However, when multiple interferences are from one identical transmitter and to a common destination, IA is not applicable under a one-DoF cost constraint. If these interfering signals are aligned in the same direction at the interfered receiver, they will also overlap with each other at their intended receiver, thus becoming indistinguishable. Moreover, IA is realized by adjusting the spatial feature of disturbance, hence incurring co-channel interference to the interfering transmission-pair's own communication. To solve this problem, we propose *cooperative IA*. Instead of adjusting the spatial characteristics of all interferences, we aim to achieve IA by adjusting interferences' strength along with one or none interference's signature, based on the interactions among multiple wireless disturbances. We propose two cooperative IA schemes: cooperative IA with space-power adjustment and cooperative IA with power adjustment. With the first method, the overall effect of all interferences is aligned in the orthogonal direction with respect to the desired signal at the interfered receiver. This method modifies the direction of one interference with a properly designed precoding vector and the strength of all interferences via power allocation. Under the second scheme, the strength of all interfering signals is modified so that the overall effect of multiple interferences is orthogonal to the desired transmission while guaranteeing the orthogonality among the interfering signals at their intended receiver. Our theoretical analysis and in-depth simulation have shown that the proposed schemes can effectively manage multiple interferences from an identical source while achieving good performance of the interfering transmission-pair.**

***Index Terms*— Interference management, interference alignment, precoding, power allocation.**

Manuscript received December 16, 2019; revised December 14, 2020, December 31, 2020, and May 5, 2021; accepted May 8, 2021. Date of publication May 21, 2021; date of current version November 11, 2021. This work was supported in part by NSF of Shaanxi Province under Grant 2021JM-143, in part by the Fundamental Research Funds for the Central Universities under Grant JB211502, in part by the Project of Key Laboratory of Science and Technology on Communication Network under Grant 6142104200412, in part by the Japan Society for the Promotion of Science (JSPS) KAKENHI under Grant JP20K14742, in part by the Project of Cyber Security Establishment with Inter University Cooperation, and in part by the U.S. National Science Foundation under Grant 1317411. The associate editor coordinating the review of this article and approving it for publication was D. Guo.

(Corresponding author: Zhao Li.)

Zhao Li is with the School of Cyber Engineering, Xidian University, Xi'an 710126, China, and also with the Science and Technology on Communication Network Laboratory, The 54th Research Institute of China Electronics Technology Group Corporation, Shijiazhuang 050081, China (e-mail: zli@xidian.edu.cn).

Jun Li, Xiujuan Liang, and Hui Li are with the School of Cyber Engineering, Xidian University, Xi'an 710126, China.

Yinghou Liu is with the School of Telecommunications Engineering, Xidian University, Xi'an 710071, China.

Kang G. Shin is with the Department of Electrical Engineering and Computer Science, University of Michigan, Ann Arbor, MI 48109 USA.

Zheng Yan is with the State Key Laboratory of ISN, Xidian University, Xi'an 710126, China, also with the School of Cyber Engineering, Xidian University, Xi'an 710126, China, and also with the Department of Communications and Networking (Comnet), Aalto University, 02150 Espoo, Finland (e-mail: zheng.yan@aalto.fi; zyan@xidian.edu.cn).

Color versions of one or more figures in this article are available at https://doi.org/10.1109/TWC.2021.3080584.

Digital Object Identifier 10.1109/TWC.2021.3080584

I. Introduction

THE emerging 5G is expected to have numerous advantages over existing communication networks [1], such as ultra-high data rate, ultra-dense connectivity, ultra low latency, etc. With the ultra-dense deployment of 5G devices and infrastructure equipment, interference will remain a main impediment to network performance. For example, about 15% more access points (APs) (due to overlapping coverage) are required for wireless voice communications so as to achieve an acceptable reception power level [2]. Although data-only communications may not require such a large amount of overlap, some coverage overlap is inevitable to achieve seamless coverage. Therefore, effective interference management is of great importance to rapidly increasing mobile users and applications. There have been various interference management schemes that can be categorized in two types. The first type is realized at the interfered transmission-pair, including the adjustment at the interfered receiver or/and its associated transmitter, e.g., zero-forcing reception [3], interference neutralization [4], [5], and interference steering [6], [7]. The second type is realized at the interfering transmitter, such as zero-forcing beamforming [8] and interference alignment (IA)[1] [11]–[14].

In all these interference management schemes, zero-forcing reception is implemented at the interfered receiver, but incurs effective signal's power loss while eliminating the interference. Both interference neutralization and interference steering are based at the interfered transmitter (associated with the interfered receiver). Interference neutralization strives to properly combine signals arriving through various paths in such a way that the interfering signals are canceled while preserving the

[1]Since many practical systems are equipped with multiple antennas which are known to greatly increase the DoFs of communication systems [9], in this paper we consider the realization of IA in multi-antenna systems without requiring symbol extensions over a very large number of time-frequency dimensions [10].

desired signals at the receiver. Although interference neutralization can mitigate interference, the power overhead of generating neutralizing signal(s) degrades the system performance as well [4], [5]. Under interference steering, a steering signal is generated to modify the propagation of interfering signal, so that the original interference is steered in the orthogonal direction of the desired transmission at the interfered receiver. In contrast with interference neutralization, interference steering focuses on the cancellation of the effective part of interference, thus becoming more power-efficient [6], [7], but requires an additional spatial DoF to place the steered interference. The authors of [7] proposed single-target interference steering and aggregated interference steering to manage multiple interferences.

However, while applying interference neutralization and interference steering, the transmitter associated with the interfered receiver needs the interference information including both the channel state information (CSI) from the interfering transmitter to the interfered receiver, and the content carried in the interference. Such information requires high-level cooperation between the interfering and interfered transmitters, hence incurring more complexity and signaling overhead. Besides, both interference neutralization and interference steering are based on interfered transmission-pair. However, it is, in practice, unfair to make the interfered transmission-pair responsible for interference management, since interference management will incur some cost such as power and DoF consumption which, in turn, results in communication performance loss, especially when the interfered side has the same or higher transmission priority than the interfering transmitter. Therefore, the interferer is amenable to participate in managing the interference(s).

As for interference management at the interfering transmitter-side, the application of zero-forcing beamforming depends on the total number of desired signals and interferences, i.e., each interfering signal component consumes one DoF [6]. In contrast, IA has been shown to be able to achieve the information-theoretic maximum DoFs in some interference networks [11], [12], and is thus a promising interference management scheme. With IA, by preprocessing the interferences at their sources, multiple interfering signals are mapped into a finite subspace at the interfered receiver to minimize the overall interference space at the unintended destination/receiver, while the desired signal(s) may be sent through a subspace without attenuation [13], [14]. IA has recently been a topic of active research. For example, the authors of [15] proposed an optimized cooperative IA scheme for a K-user multiple-input multiple-output (MIMO) interference channel [16,17], where K user-pairs interfere with each other. This scheme requires CSI sharing among base stations, making its implementation expensive and complex. The authors of [18] presented a downlink interference management scheme based on the cooperation among a number of multiple interfering femtocells. Like other IA schemes, the downlink transmission in these femtocells would be sacrificed. An interference alignment and neutralization based coordinated multi-point transmission was proposed for a typical MIMO X channel [14] forming two interfering communication pairs, and then extended to more general situations in [19]. By incorporating both IA and interference neutralization and exploiting their advantages in interference management, effective interference cancellation and suppression can be achieved.

Of the above-mentioned IA schemes, [11]–[15], [17], [18] require the transmitters to cooperate with each other so as to align multiple interferences from the same source in a multi-dimensional subspace (i.e., more than one DoF is used for IA) at the interfered receiver. However, there may be limited DoFs available for IA. Moreover, given multiple interferences from an identical transmitter and to a common receiver, if the disturbances are aligned in an identical direction at the interfered receiver, i.e., incurring only one DoF cost, these aligned interferences will also overlap with each other at their common destination, thus becoming indistinguishable [19]. Although [19] incorporates IA and interference neutralization to overcome the limitations of applying single interference management method and achieves some benefits, it incurs both DoF and power costs.

Based on the above discussion, effective management of multiple interferences from the same source with little or no transmitter-side cooperation overhead [11]–[19], transmit power consumption [4]–[7], [19] at the interfered transmitter, interfered receiver-side DoF cost, as well as performance loss of interfering transmission-pair, is of great importance to emerging ultra-dense wireless networks. To meet this need, we propose a novel interference management method called *cooperative interference alignment* (i.e., cooperative IA). By exploiting interactions among multiple interfering signals, the overall effect of the interferences is aligned to be orthogonal to the desired signal at the interfered receiver by either adjusting the spatial feature of a single interference and the strength of all the disturbances, or modifying the transmit power of all interferences without changing their spatial characteristics. The proposed cooperative IA is realized at the interfering transmitter, and hence based only on the CSI. Besides, cooperative IA does not cost transmit power and consumes only one DoF for interference management at the interfered receiver-side. In addition, cooperative IA can manage not only the disturbances from the same source, but also those from different sources.

The contributions of this paper are two-fold:

- Proposal of cooperative IA via adjustment of the spatial feature of one interference and the strength of all disturbances, named as *cooperative IA with space-power adjustment* (CIA-SPA). With CIA-SPA, the overall effect of all interferences is aligned in the orthogonal direction with respect to the desired signal at the interfered receiver.
- Development of *cooperative IA with power adjustment* (CIA-PA). By re-allocating the transmit power for all interfering signals, the overall effect of multiple interferences can be orthogonal to the desired transmission at the interfered receiver while guaranteeing the orthogonality among the interfering signals at their intended receiver. Therefore, no co-channel interference among the multiple beams of the interfering transmission-pair is incurred.

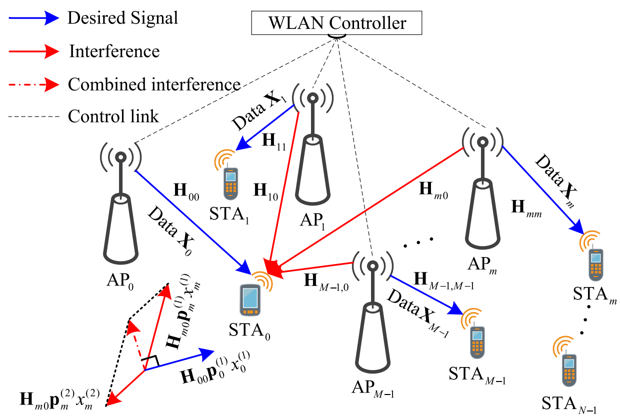

Fig. 1. System model.

The rest of this paper is organized as follows. Section II describes the system model, while Section III details the CIA-SPA and CIA-PA. Then, Section IV evaluates their performance. Finally, Section V concludes the paper.

In the rest of this paper, we will use the following notations. The set of complex numbers is denoted as $\mathbb{C}$, while vectors and matrices are represented by bold letters. Let $\mathbf{X}^T$, $\mathbf{X}^H$, $\mathbf{X}^\dagger$ and $\det(\mathbf{X})$ denote the transpose, Hermitian, pseudo inverse and determinant of matrix $\mathbf{X}$, respectively. $\|\cdot\|$ and $|\cdot|$ indicate the Euclidean norm and the absolute value. $\mathbb{E}(\cdot)$ denotes statistical expectation and $\langle \mathbf{a}, \mathbf{b} \rangle$ represents the inner product of two vectors.

II. System Model

We consider downlink communications in an infrastructure-based enterprise wireless local area network (WLAN) in which coverage areas of access points often overlap. Fig. 1 shows M adjacent basic service sets (BSSs) with overlapping coverage areas. All APs are assumed to use the same transmit power, P_T, which is referred to as *transmit power constraint* in the following discussion, and connected to a central WLAN controller so that downlink transmissions from APs to their clients/stations (STAs) are synchronized. For the purpose of enhancing spectral efficiency, we may reuse spectrum more aggressively with effective interference management. In such a case, co-channel interference may occur between adjacent BSSs. In practice, there may be multiple communication links between an AP and its serving STAs. In such a case, the AP can employ a proper scheduling algorithm [20] to select a set of users from all of its candidate STAs to serve, and then assign each STA an exclusive channel so as to avoid co-channel interference between the transmissions from an associated AP to its serving STAs. Therefore, we need to consider and manage only those transmissions sharing the same channel resource in adjacent coverage areas of various APs and interferences among these transmissions, as shown in Fig. 1. Based on this observation, although multiple STAs may exist in an AP's coverage area, only one STA is served at a time by its associated AP via one frequency channel and each STA is associated with one AP at a time. Suppose there are N STAs and M APs in the system. Then, $M \leq N$ because we deal with interference management in one channel shared by multiple adjacent AP–STA pairs where each STA is scheduled by its associated AP. Let STA$_n$ ($n \in \{0, 1, \cdots, N-1\}$) and AP$_m$ ($m \in \{0, 1, \cdots, M-1\}$) denote the mobile user and the AP indexed by n and m, respectively. Since an AP serves only one STA at a time, we let STA$_m$ represent the scheduled and served STA which is associated with AP$_m$. Given a certain frequency channel, an AP serves only one STA at a time; this STA is interfered with by adjacent APs using the same channel. Therefore, we show in Fig. 1 the AP–STA pairs using the same channel resource, a scheduled STA, e.g., STA$_0$, is interfered with by its adjacent APs using the same channel; whereas for the other STAs, they are assigned different channels, hence causing no co-channel interference.

Each AP and STA is assumed to be equipped with N_T and N_R antennas, respectively. Since mobile stations/devices are subject to more cost and hardware restrictions than an AP, we let $N_T \geq N_R$. $\mathbf{H}_{mn} \in \mathbb{C}^{N_R \times N_T}$ denote the spatial channel from AP$_m$ to STA$_n$. We employ a spatially uncorrelated Rayleigh flat fading channel model so that the elements of $\mathbf{H}_{mn}$ are modeled as independent and identically distributed zero-mean unit-variance complex Gaussian random variables. All users experience block fading, i.e., channel parameters in a block consisting of several successive transmission cycles remain constant in the block and vary randomly between blocks. Each STA can accurately estimate CSI with respect to its intended and nearby unintended APs [21], [22] and report the CSI to its associated AP via a low-rate, error-free link. Then, APs can share CSI and their transmitted data with each other via a central controller. A STA should, in practice, be able to tell the collision caused by co-channel interference from fading individually [23] or cooperatively [24] with its associated AP, so that the interfered STA can inform its associated AP to request the WLAN controller for assistance. Then, the controller checks its database against this request and finds an interference-management solution. The above steps are consistent with the centralized management (a.k.a. centralized radio access network, C-RAN) proposed in 5G [25], where high-level management nodes may be defined to be responsible for all information.

Let $\mathbf{X}_m = [x_m^{(1)} \; \cdots \; x_m^{(k)} \; \cdots \; x_m^{(K)}]$ be the desired data vector from AP$_m$ to its currently serving client STA$_m$. $\mathbb{E}(\|x_m^{(k)}\|^2) = 1$ holds. Without loss of generality, we let AP$_0$ and STA$_0$ be the interfered transmission-pair, and AP$_1$ and STA$_1$ be the interfering transmission-pair. For clarity of presentation, we assume AP$_1$ sends $\mathbf{X}_1 = [x_1^{(1)} \; \cdots \; x_1^{(k)} \; \cdots \; x_1^{(K)}]$, each element of $\mathbf{X}_1$ is carried by one of the K concurrent signals. AP$_0$ sends G desired signals carrying $\mathbf{X}_0 = [x_0^{(1)} \; \cdots \; x_0^{(g)} \; \cdots \; x_0^{(G)}]$ to STA$_0$. The numbers of antennas of receivers and transmitters need to satisfy $N_T = N_R \geq \max\{K, G+1\}$. For simplicity, we assume all the interfering signals employ the same modulation scheme. However, given different modulation schemes adopted by various signals, the following analysis can be directly applied. Since each element in the modulation symbol set can be determined by its amplitude and phase information, all symbols in the symbol set can be represented by one referential symbol [26]. Therefore, one can select an arbitrary referential symbol, then the data carried in an arbitrary signal can be represented in terms of this referential symbol [26]. Without loss of generality, we take $x_1^{(\hat{k})} = \alpha_{\hat{k}} e^{j\theta^{(\hat{k})}}$ ($\hat{k} \in \{1, 2, \cdots, K\}$) as the referential symbol, then an arbitrary symbol $x_1^{(k)} = \alpha_k e^{j\theta^{(k)}}$ ($k \in \{1, 2, \cdots, K\}$ and $k \neq \hat{k}$) can be expressed as $x_1^{(k)} = a_k x_1^{(\hat{k})}$. Both $x_1^{(\hat{k})}$ and $x_1^{(k)}$ belong to a finite modulation symbol set. We can get $a_k = \frac{\alpha_k}{\alpha_{\hat{k}}} e^{j(\theta_k - \theta_{\hat{k}})}$ where α_k, $\alpha_{\hat{k}}$, θ_k and $\theta_{\hat{k}}$ are the amplitudes and phases of $x_1^{(k)}$ and $x_1^{(\hat{k})}$, respectively. Since wireless signals interact with each other during their propagation, and the data symbols carried in signals can be mutually represented, the overall effect of interferences to STA_0 can be expressed by an effective interference carrying data $x_1^{(\hat{k})}$.

III. Main Results and Discussion

This section details the design of cooperative interference alignment based on the interactions among multiple interfering signals. We present two realizations of cooperative IA under a fixed transmit power constraint, P_T, at the interfering transmitter. The first is CIA-SPA, with which only one interference's spatial signature is adjusted by adopting proper precoding vector, and then the transmit power for all disturbances is modified. The second one is CIA-PA, with which all interferences' strength is adjusted while keeping their spatial characteristics intact. Both schemes can align the overall effect of all disturbances in the orthogonal direction with respect to the desired transmission of the interfered receiver.

A. Design of CIA-SPA

When AP_1 sends K signals causing interference to the G signals from AP_0 to STA_0, the mixed signals received by STA_0 and STA_1 can be expressed as:

$$\mathbf{y}_0 = \sqrt{\frac{P_T}{G}} \sum_{g=1}^{G} \mathbf{H}_{00} \mathbf{p}_0^{(g)} x_0^{(g)} + \sqrt{\frac{P_T}{K}} \sum_{k=1}^{K} \mathbf{H}_{10} \mathbf{p}_1^{(k)} x_1^{(k)} + \mathbf{n}_0 \tag{1}$$

and

$$\mathbf{y}_1 = \sqrt{\frac{P_T}{K}} \sum_{k=1}^{K} \mathbf{H}_{11} \mathbf{p}_1^{(k)} x_1^{(k)} + \mathbf{n}_1 \tag{2}$$

where P_T denotes the transmit power of AP. Equal power allocation is adopted by both APs. That is, P_T is equally allocated to either G desired signals or K interferences. Although optimal power allocation, such as waterfilling algorithm [3], can be employed to maximize the achievable spectral efficiency, since the proposed cooperative IA schemes are realized by adjusting the interfering signals' power, the optimality of power allocation over multiple transmissions cannot be guaranteed. Moreover, we focus on the design of cooperative IA to overcome the limitation of traditional IA in managing multiple interferences from the same source, rather than achieving the performance gain via optimal power allocation, and hence we do not consider optimal power allocation. $\mathbf{p}_0^{(g)}$ ($g \in \{1, \cdots, G\}$) and $\mathbf{p}_1^{(k)}$ ($k \in \{1, \cdots, K\}$) are the precoders of data symbols $x_0^{(g)}$ and $x_1^{(k)}$ sent by AP_0 and AP_1, respectively, $\mathbf{H}_{mn}$ ($m, n \in \{0, 1\}$) is the channel matrix from AP_m to STA_n. The first term on the right-hand side of Eq. (1) represents the desired signal of STA_0, while the second term denotes the total interference from AP_1. The k-th interfering component is $\mathbf{i}^{(k)} = \sqrt{\frac{P_T}{K}} \mathbf{H}_{10} \mathbf{p}_1^{(k)} x_1^{(k)}$. As for Eq. (2), the first term on the right-hand side is the desired signal of STA_1. $\mathbf{n}_i$ ($i \in \{0, 1\}$) denotes the additive white Gaussian noise vector with zero-mean and variance σ_n^2. $\mathbb{E}(\mathbf{n}_i \mathbf{n}_i^H) = \sigma_n^2 \mathbf{I}_{N_R}$ holds where $\mathbf{I}_{N_R}$ is an $N_R \times N_R$ unit matrix.

We employ singular value decomposition based precoding and receive filtering as an example. By applying singular value decomposition to $\mathbf{H}_{mn}$, we can have $\mathbf{H}_{mn} = \mathbf{U}_{mn} \mathbf{\Sigma}_{mn} \mathbf{V}_{mn}^H$ where $\mathbf{V}_{mn} = [\mathbf{v}_{mn}^{(1)} \cdots \mathbf{v}_{mn}^{(N_T)}]$ and $\mathbf{U}_{mn} = [\mathbf{u}_{mn}^{(1)} \cdots \mathbf{u}_{mn}^{(N_R)}]$. The column vectors of $\mathbf{V}_{mn}$ and $\mathbf{U}_{mn}$ indicate the spatial signatures of the sub-channels. The non-zero elements on the main diagonal of matrix $\mathbf{\Sigma}_{mn}$, arranging in descending order, represent the amplitude gain of the spatial sub-channel. $\mathbf{v}_{mn}^{(1)}$ and $\mathbf{u}_{mn}^{(1)}$ are the first column vectors of the right and left singular matrices $\mathbf{V}_{mn}$ and $\mathbf{U}_{mn}$, respectively, corresponding to the principal eigenmode of $\mathbf{H}_{mn}$. AP_0 and AP_1 choose precoding matrices $\mathbf{P}_0 = [\mathbf{p}_0^{(1)} \cdots \mathbf{p}_0^{(g)} \cdots \mathbf{p}_0^{(G)}]$ and $\mathbf{P}_1 = [\mathbf{p}_1^{(1)} \cdots \mathbf{p}_0^{(k)} \cdots \mathbf{p}_0^{(K)}]$ where $\mathbf{p}_0^{(g)} = \mathbf{v}_{00}^{(g)}$ ($g \in \{1, 2, \cdots, G\}$) and $\mathbf{p}_1^{(k)} = \mathbf{v}_{11}^{(k)}$ ($k \in \{1, 2, \cdots, K\}$). STA_0 and STA_1 employ filter matrices $\mathbf{F}_0 = [\mathbf{f}_0^{(1)} \cdots \mathbf{f}_0^{(g)} \cdots \mathbf{f}_0^{(G)}]$ and $\mathbf{F}_1 = [\mathbf{f}_1^{(1)} \cdots \mathbf{f}_1^{(k)} \cdots \mathbf{f}_1^{(K)}]$ where $\mathbf{f}_0^{(g)} = \mathbf{u}_{00}^{(g)}$ and $\mathbf{f}_1^{(k)} = \mathbf{u}_{11}^{(k)}$.

Since wireless signals interact with each other during their propagation, and the data symbols carried in signals can be mutually represented, the overall effect of interferences to STA_0 can be obtained as:

$$\mathbf{i}^{(\Sigma)} = \sqrt{\frac{P_T}{K}} \sum_{k=1}^{K} \mathbf{H}_{10} \mathbf{p}_1^{(k)} x_1^{(k)} = \sqrt{\frac{P_T}{K}} \sum_{k=1}^{K} \mathbf{H}_{10} \mathbf{p}_1^{(k)} a_k x_1^{(\hat{k})}. \tag{3}$$

where $x_1^{(\hat{k})}$ ($\hat{k} \in \{1, 2, \cdots, K\}$) is the referential symbol that can be arbitrarily selected. A detailed explanation can be found in the system model part.

In what follows, we will present the design of CIA-SPA. In order to eliminate the influence of multiple interferences on the desired transmission at STA_0, we appropriately design the precoding vector of one interference, say $\mathbf{i}^{(k^*)} = \sqrt{\frac{P_T}{K}} \mathbf{H}_{10} \mathbf{p}_1^{(k^*)} x_1^{(k^*)}$ ($k^* \in \{1, 2, \cdots, K\}$), and the strength of all interferences. Since the precoding vector of the selected interference is designed for the alignment of the overall effect of all disturbances at the interfered receiver, the transmission of this interfering signal no longer matches its data channel, i.e., $\mathbf{H}_{11}$. That is, the transmission performance of the interfering signal whose precoder is designed in terms of CIA-SPA is sacrificed. Moreover, the orthogonality between $\sqrt{\frac{P_T}{K}} \mathbf{H}_{11} \mathbf{p}_1^{(k^*)} x_1^{(k^*)}$ and $\sqrt{\frac{P_T}{K}} \mathbf{H}_{11} \mathbf{p}_1^{(k)} x_1^{(k)}$ ($k, k^* \in \{1, 2, \cdots, K\}$ and $k \neq k^*$) is no longer guaranteed, thus causing co-channel interference. However, the transmissions of

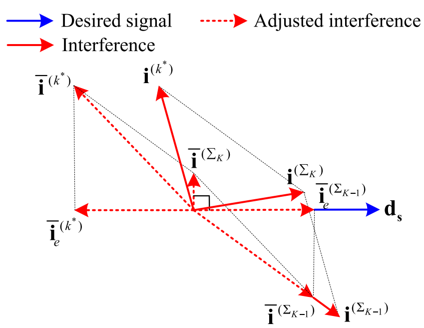

Fig. 2. An illustration of CIA-SPA under K interferences and one desired signal. An interference $\mathbf{i}^{(k^*)}$ is selected and preprocessed to become $\bar{\mathbf{i}}^{(k^*)}$. Then, the remaining $K-1$ interferences are adjusted so that their overall effect $\mathbf{i}^{(\Sigma_{K-1})}$ becomes $\bar{\mathbf{i}}^{(\Sigma_{K-1})}$, satisfying that the projection of $\bar{\mathbf{i}}^{(\Sigma_{K-1})}$ on the direction of desired signal, $\mathbf{d}_\mathbf{s}$, denoted as $\bar{\mathbf{i}}_e^{(\Sigma_{K-1})}$, is of the same strength and opposite direction with respect to the projection of $\bar{\mathbf{i}}^{(k^*)}$ on $\mathbf{d}_\mathbf{s}$, i.e., $\bar{\mathbf{i}}_e^{(k^*)}$. Therefore, the overall effect of K interferences after realizing CIA-SPA, i.e., $\bar{\mathbf{i}}^{(\Sigma_K)}$, is aligned in the orthogonal direction with respect to the desired transmission at STA_0.

the remaining $K-1$ disturbances to their desired receiver still match $\mathbf{H}_{11}$, hence achieving good transmission performance.

Fig. 2 shows the principle of CIA-SPA under one desired transmission and K interferences. Without loss of generality, we select the k^*-th interference and design its precoding vector. The k^*-th interference with new precoder becomes:

$$\bar{\mathbf{i}}^{(k^*)} = \sqrt{\frac{P_T}{K}\varepsilon_{k^*}}\mathbf{H}_{10}\overline{\mathbf{p}}_1^{(k^*)}x_1^{(k^*)} \tag{4}$$

where $\varepsilon_{k^*} \in (0, K)$ denotes the power coefficient. $\overline{\mathbf{p}}_1^{(k^*)}$ is the designed precoding vector for adjusting $\mathbf{i}^{(k^*)}$. $\|\overline{\mathbf{p}}_1^{(k^*)}\| = 1$ holds.

Since the transmit power for the interference indexed by k^* has been modified to $\frac{P_T}{K}\varepsilon_{k^*}$, in order to satisfy the total transmit power constraint, P_T, at the interference source, the power used for the rest $K-1$ interfering signals should be re-allocated. So, the k-th interference of the remaining $K-1$ disturbances with power adjustment is given as:

$$\bar{\mathbf{i}}^{(k)} = \sqrt{\frac{P_T}{K}\varepsilon_k}\mathbf{H}_{10}\mathbf{p}_1^{(k)}x_1^{(k)} \tag{5}$$

where $\varepsilon_k \in (0, K)$ denotes the power allocation factor for interference $\mathbf{i}^{(k)}$ where $k \neq k^*$.

From Eq. (3) we can rewrite Eqs. (4) and (5) as $\bar{\mathbf{i}}^{(k^*)} = \sqrt{\frac{P_T}{K}\varepsilon_{k^*}}\mathbf{H}_{10}\overline{\mathbf{p}}_1^{(k^*)}a_{k^*}x_1^{(\hat{k})}$ and $\bar{\mathbf{i}}^{(k)} = \sqrt{\frac{P_T}{K}\varepsilon_k}\mathbf{H}_{10}\mathbf{p}_1^{(k)}a_k x_1^{(\hat{k})}$, respectively, where $x_1^{(\hat{k})}$ is the referential symbol. Then, $\bar{\mathbf{i}}^{(k^*)}$ and $\bar{\mathbf{i}}^{(k)}$ become two interfering components carrying the same data $x_1^{(\hat{k})}$. With CIA-SPA, the overall effect of all interferences should be adjusted to the orthogonal direction with respect to the desired transmission(s) at STA_0. That is, projections of $\bar{\mathbf{i}}^{(k^*)}$ and $\sum_{k=1,k\neq k^*}^{K}\bar{\mathbf{i}}^{(k)}$ on the subspace determined by the G desired signals from AP_0 to STA_0, denoted by $\mathcal{G}$, should counteract with each other, so that only the orthogonal components with respect to $\mathcal{G}$ are left. Then, we can have Eq. (6), shown at the bottom of the page.

$\mathbf{W}_\mathcal{G}$ is the projection matrix with respect to $\mathcal{G}$. We define $\mathbf{W}_g = \mathbf{d}_{\mathbf{s}^{(g)}}(\mathbf{d}_{\mathbf{s}^{(g)}}^H\mathbf{d}_{\mathbf{s}^{(g)}})^{-1}\mathbf{d}_{\mathbf{s}^{(g)}}^H$ $(g \in \{1, 2, \cdots, G\})$ to denote the projection matrix with respect to the desired signal $\mathbf{s}^{(g)} = \sqrt{\frac{P_T}{G}}\mathbf{H}_{00}\mathbf{p}_0^{(g)}x_0^{(g)}$, and $\mathbf{d}_{\mathbf{s}^{(g)}} = \frac{\mathbf{H}_{00}\mathbf{p}_0^{(g)}}{\|\mathbf{H}_{00}\mathbf{p}_0^{(g)}\|}$ is the direction of $\mathbf{s}^{(g)}$. Then, we have $\mathbf{W}_\mathcal{G} = \sum_{g=1}^{G}\mathbf{W}_g$. The left-hand side and right-hand side of Eq. (6) represent for the projection of $\bar{\mathbf{i}}^{(k^*)}$ and the overall effect of the remaining $K-1$ interferences except for $\mathbf{i}^{(k^*)}$, i.e., $\bar{\mathbf{i}}^{(\Sigma_{K-1})}$, on $\mathcal{G}$. $a_{k^*} = \frac{\alpha_{k^*}}{\alpha_{\hat{k}}}e^{j(\theta_{k^*}-\theta_{\hat{k}})}$, α_{k^*} and θ_{k^*} are the amplitude and phase of $x_1^{(k^*)}$.

Then, we can have Lemma 1 as follows.

Lemma 1: By employing precoding vector $\overline{\mathbf{p}}_1^{(k^*)}$ and the power coefficients set as given in Eqs. (7)–(9), respectively:

$$\overline{\mathbf{p}}_1^{(k^*)} = \frac{1}{r}\left\{-(\mathbf{W}_\mathcal{G}\mathbf{H}_{10}a_{k^*})^\dagger\mathbf{W}_\mathcal{G}\mathbf{H}_{10}\sum_{k=1,k\neq k^*}^{K}\mathbf{p}_1^{(k)}a_k\right\}, \tag{7}$$

$$\varepsilon_{k^*} = \frac{Kr^2}{K-1+r^2}, \tag{8}$$

$$\varepsilon_k = \frac{K}{K-1+r^2} \tag{9}$$

where $r = \| - (\mathbf{W}_\mathcal{G}\mathbf{H}_{10}a_{k^*})^\dagger\mathbf{W}_\mathcal{G}\mathbf{H}_{10}\sum_{k=1,k\neq k^*}^{K}\mathbf{p}_1^{(k)}a_k\|$, CIA-SPA can be realized.

The proof of Lemma 1 is given in Appendix A.

From Eqs. (8)–(9) and (23) we can get $\varepsilon_{k^*} \in (0, K)$ and $\varepsilon_k \in (0, \frac{K}{K-1})$. In the case of $\mathbf{i}^{(k^*)}$ being orthogonal to $\mathbf{d}_\mathbf{s}$, ε_{k^*} is as large as K and ε_k becomes 0. In such a case, $\mathbf{i}^{(k^*)}$ is allocated power P_T whereas the other $K-1$ interfering transmissions are shut off, making CIA-SPA inapplicable. Therefore, to use CIA-SPA, the qualification of ε_{k^*} and ε_k should be verified. That is, if either the selected $\mathbf{i}^{(k^*)}$ or $\mathbf{i}^{(\Sigma_{K-1})}$ is orthogonal to $\mathbf{d}_\mathbf{s}$, the left-hand side or the right-hand side of Eq. (6) becomes $\mathbf{0}$, yielding the solution for ε_k or ε_{k^*} becomes 0; in such a case, another interference should be selected as $\mathbf{i}^{(k^*)}$ for computing qualified ε_{k^*} and ε_k. Note that there exists at least one $\mathbf{i}^{(k^*)}$ being non-orthogonal to $\mathbf{d}_\mathbf{s}$ so as to obtain qualified ε_{k^*} and ε_k; otherwise, all interfering components are located in the orthogonal subspace with respect to $\mathbf{d}_\mathbf{s}$, thus unneeding interference management.

Based on the above discussion, the received signals at STA_0 and STA_1 are given by Eqs. (10)–(11), shown at the bottom of the next page.

We employ $\mathbf{F}_0 = [\mathbf{f}_0^{(1)} \ \cdots \ \mathbf{f}_0^{(g)} \ \cdots \ \mathbf{f}_0^{(G)}]$ and $\mathbf{F}_1 = [\mathbf{f}_1^{(1)} \ \cdots \ \mathbf{f}_1^{(k^*)} \ \cdots \ \mathbf{f}_1^{(K)}]$ as the filter matrices at STA_0 and STA_1, respectively. They can be obtained by applying

$$\mathbf{W}_\mathcal{G}\sqrt{\frac{P_T}{K}\varepsilon_{k^*}}\mathbf{H}_{10}\overline{\mathbf{p}}_1^{(k^*)}a_{k^*}x_1^{(\hat{k})} = -\mathbf{W}_\mathcal{G}\sum_{k=1,k\neq k^*}^{K}\sqrt{\frac{P_T}{K}\varepsilon_k}\mathbf{H}_{10}\mathbf{p}_1^{(k)}a_k x_1^{(\hat{k})} \tag{6}$$

singular value decomposition to $\mathbf{H}_{00}$ and $\mathbf{H}_{11}$, respectively. Then, we left-multiply the received signals $\mathbf{y}_0^{CIA-SPA}$ and $\mathbf{y}_1^{CIA-SPA}$ by $\mathbf{F}_0^H$ and $\mathbf{F}_1^H$, at STA_0 and STA_1, respectively, to recover G and K signal components. So, spectral efficiency of STA_0 and STA_1 can be calculated according to Eqs. (12)–(13), shown at the bottom of the page, where $\lambda_{00}^{(1)}$ and $\lambda_{11}^{(1)}$ denote the largest singular values of $\mathbf{H}_{00}$ and $\mathbf{H}_{11}$, and $\lambda_{00}^{(g)}$ and $\lambda_{11}^{(k)}$ are the gth and kth singular values of $\mathbf{H}_{00}$ and $\mathbf{H}_{11}$, respectively. $\frac{P_T}{K}\varepsilon_{k^*}\|[\mathbf{f}_1^{(k)}]^H\mathbf{H}_{11}\overline{\mathbf{p}}_1^{(k^*)}\|^2$ represents the co-channel interference incurred by the k^*th adjusted signal component of transmission-pair AP_1–STA_1 to its other signal indexed by k.

B. Design of CIA-PA

CIA-SPA presented in the previous subsection adjusts the spatial signature of one of K interferences. Therefore, this direction-adjusted disturbance, also acting as a desired signal of its own transmission-pair (i.e., the interfering AP_1 and STA_1), is no longer orthogonal to the other signals from AP_1 to STA_1, incurring co-channel interference and loss of communication quality of the interfering transmission-pair.

Here we will propose another scheme called CIA-PA. By multiplying a complex coefficient to each interference component, the overall effect of all interferences becomes orthogonal to the desired signal at the interfered receiver. Since CIA-PA only adjusts all interferences' strength without changing their spatial characteristics, no co-channel interference is introduced. CIA-PA consists of two-phase adjustments. In the first phase, only part of interferences' strength is adjusted to confine the overall effect of interferences to the orthogonal subspace of the desired transmission. In the second phase, the strength of all disturbances is adjusted in proportion to their intensity after the first-phase adjustment so as to satisfy the transmit power constraint, P_T, at the interfering transmitter.

Fig. 3 illustrates the principle of CIA-PA under $K \geq 3$ and $G = 2$, where vectors $\mathbf{d}_{\mathbf{s}^{(1)}}$ and $\mathbf{d}_{\mathbf{s}^{(2)}}$ denote the spatial features of the two desired signals of the interfered transmission-pair. They determine a two-dimensional signal subspace denoted by $\mathcal{G}$. For simplicity, we group K interferences in three sets, i.e., $\{\mathbf{i}^{(k_1)}\}$, $\{\mathbf{i}^{(k_2)}\}$ and $\{\mathbf{i}^{(k)}\}$ where $k_1, k_2, k \in \{1, 2, \cdots, K\}$ and $k_1 \neq k_2 \neq k$. $\{\mathbf{i}^{(k)}\}$ has $K-2$ elements. We can have $\mathbf{i}_e^{(k_i)} = \sum_{g=1}^{2}\mathbf{W}_g\sqrt{\frac{P_T}{K}}\mathbf{H}_{10}\mathbf{p}_1^{(k_i)}a_{k_i}x_1^{(\hat{k})}$

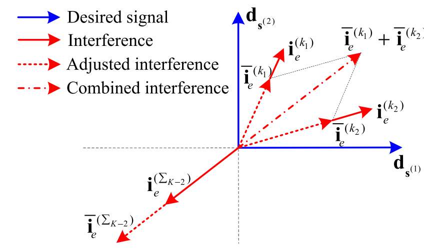

Fig. 3. An illustration of CIA-PA under $K \geq 3$ and $G = 2$. Interferences $\mathbf{i}^{(k_1)}$ and $\mathbf{i}^{(k_2)}$ are adjusted so that their projections on the desired signals subspace determined by vectors $\mathbf{d}_{\mathbf{s}^{(1)}}$ and $\mathbf{d}_{\mathbf{s}^{(2)}}$, denoted by $\mathbf{i}_e^{(k_1)}$ and $\mathbf{i}_e^{(k_2)}$, become $\overline{\mathbf{i}}_e^{(k_1)}$ and $\overline{\mathbf{i}}_e^{(k_2)}$, respectively. Then, the remaining $K-2$ interferences are adjusted so that their overall effect $\mathbf{i}_e^{(\Sigma_{K-2})}$ becomes $\overline{\mathbf{i}}_e^{(\Sigma_{K-2})}$. With CIA-PA, $\overline{\mathbf{i}}_e^{(\Sigma_{K-2})}$ is of the same strength and opposite direction with respect to $\overline{\mathbf{i}}_e^{(k_1)} + \overline{\mathbf{i}}_e^{(k_2)}$, thus causing no interference in the desired signals subspace.

($i \in \{1, 2\}$), representing for the projection of $\mathbf{i}^{(k_i)}$ on $\mathcal{G}$. $\mathbf{W}_g$ denotes the projection matrix with respect to the g-th desired signal. As for the remaining $K-2$ disturbances, we consider the projection of their overall effect on $\mathcal{G}$, i.e., $\mathbf{i}_e^{(\sum_{K-2})} = \sum_{g=1}^{2}\mathbf{W}_g\sum_{k=1,k\notin\{k_1,k_2\}}^{K}\sqrt{\frac{P_T}{K}}\mathbf{H}_{10}\mathbf{p}_1^{(k)}a_k x_1^{(\hat{k})}$. Similarly, we use $\overline{\mathbf{i}}_e^{(k_i)}$ and $\overline{\mathbf{i}}_e^{(\sum_{K-2})}$ to denote the adjusted interferences' projections on $\mathcal{G}$.

CIA-PA adjusts the length of vectors $\mathbf{i}^{(k_i)}$ and $\mathbf{i}^{(\sum_{K-2})}$ by multiplying a proper complex coefficient to each of them, so that $\sum_{i=1}^{2}\overline{\mathbf{i}}_e^{(k_i)} + \overline{\mathbf{i}}_e^{(\sum_{K-2})} = \mathbf{0}$ holds. That is, the projections of all adjusted interferences on $\mathcal{G}$ interact with each other so that the effective interference becomes zero. However, it should be noted that there exists an effect of all disturbances (we can also call it *residual effective interference* without ambiguity) orthogonal to $\mathcal{G}$; this residual effect consumes one DoF at the interfered receiver, similarly to that of IA. Since CIA-PA does not modify interferences' spatial features, the orthogonality among K concurrent transmissions from AP_1 to STA_1 is preserved.

We now detail the realization of CIA-PA. For clarity of exposition, we begin our design with $G = 2$. However, the proposed method can be easily extended to the case of $G > 2$. First, we divide K interferences in three groups, denoted by $\{\mathbf{i}^{(k_1)}\}$, $\{\mathbf{i}^{(k_2)}\}$ and $\{\mathbf{i}^{(k)}\}$ where $k_1, k_2, k \in \{1, 2, \cdots, K\}$, and $k_1 \neq k_2 \neq k$ as mentioned above. Note that $\{\mathbf{i}^{(k)}\}$

$$\mathbf{y}_0^{CIA-SPA} = \sqrt{\frac{P_T}{G}}\sum_{g=1}^{G}\mathbf{H}_{00}\mathbf{p}_0^{(g)}x_0^{(g)} + \sqrt{\frac{P_T}{K}\varepsilon_{k^*}}\mathbf{H}_{10}\overline{\mathbf{p}}_1^{(k^*)}x_1^{(k^*)} + \sqrt{\frac{P_T}{K}\varepsilon_k}\sum_{k=1,k\neq k^*}^{K}\mathbf{H}_{10}\mathbf{p}_1^{(k)}x_1^{(k)} + \mathbf{n}_0 \tag{10}$$

$$\mathbf{y}_1^{CIA-SPA} = \sqrt{\frac{P_T}{K}\varepsilon_{k^*}}\mathbf{H}_{11}\overline{\mathbf{p}}_1^{(k^*)}x_1^{(k^*)} + \sqrt{\frac{P_T}{K}\varepsilon_{k^*}}\sum_{k=1,k\neq k^*}^{K}\mathbf{H}_{11}\mathbf{p}_1^{(k)}x_1^{(k)} + \mathbf{n}_1 \tag{11}$$

$$c_0^{CIA-SPA} = \log_2\{\det(\mathbf{I}_G + \frac{P_T}{\sigma_n^2}\mathbf{F}_0^H\mathbf{H}_{00}\mathbf{P}_0\mathbf{X}_0)\} = \sum_{g=1}^{G}\log_2\{1 + \frac{P_T}{G\sigma_n^2}[\lambda_{00}^{(g)}]^2\} \tag{12}$$

$$c_1^{CIA-SPA} = \log_2\{1 + \frac{P_T}{K\sigma_n^2}\varepsilon_{k^*}\}\|[\mathbf{f}_1^{(k^*)}]^H\mathbf{H}_{11}\overline{\mathbf{p}}_1^{k^*}\|^2 + \sum_{k=1,k\neq k^*}^{K}\log_2\left\{1 + \frac{\frac{P_T}{K}\varepsilon_k[\lambda_{11}^{(k)}]^2}{\frac{P_T}{K}\varepsilon_{k^*}\|[\mathbf{f}_1^{(k)}]^H\mathbf{H}_{11}\overline{\mathbf{p}}_1^{(k^*)}\|^2 + \sigma_n^2}\right\} \tag{13}$$

contains $K-2$ interfering components. By exploiting interactions among multiple signals, we can obtain the effect of $K-2$ interferences, i.e., except for $\mathbf{i}^{(k_i)}$ ($i \in \{1,2\}$), as $\mathbf{i}^{(\sum_{K-2})}$. The projections of $\mathbf{i}^{(k_i)}$ and $\mathbf{i}^{(\sum_{K-2})}$ on $\mathcal{G}$ determined by $\{\mathbf{s}^{(g)}\}$ ($g \in \{1, 2, \cdots, G\}$) are denoted by $\mathbf{i}_e^{(k_i)}$ and $\mathbf{i}_e^{(\sum_{K-2})}$, respectively.

Then, we multiply $\mathbf{i}^{(k_1)}$, $\mathbf{i}^{(k_2)}$ and $\mathbf{i}^{(\sum_{K-2})}$ by three designed complex coefficients, respectively, so that the projections of the adjusted interferences on $\mathcal{G}$ are obtained as $\bar{\mathbf{i}}_e^{(k_1)}$, $\bar{\mathbf{i}}_e^{(k_2)}$ and $\bar{\mathbf{i}}_e^{(\sum_{K-2})}$. We can have:

$$\mathbf{i}_e^{(k_i)} = \mathbf{W}_1 \mathbf{i}^{(k_i)} + \mathbf{W}_2 \mathbf{i}^{(k_i)}, \tag{14}$$

$$\mathbf{i}_e^{(\sum_{K-2})} = \mathbf{W}_1 \mathbf{i}^{(\sum_{K-2})} + \mathbf{W}_2 \mathbf{i}^{(\sum_{K-2})} \tag{15}$$

where $i \in \{1,2\}$. Note that when the designed coefficient is applied to the effective interference $\mathbf{i}^{(\sum_{K-2})}$, the same coefficient should be multiplied by each of the $K-2$ interferences.

We can arbitrarily select two of the three interference groups for the first-phase adjustment. Here we take $\mathbf{i}^{(k_1)}$ and $\mathbf{i}^{(k_2)}$ for simplicity, and provide Lemma 2 as follows.

Lemma 2: By employing coefficients $\sqrt{\chi \rho_{(k_1)}^2} \beta_{(k_1)}$, $\sqrt{\chi \rho_{(k_2)}^2} \beta_{(k_2)}$ and $\sqrt{\chi}$ for adjusting $\mathbf{i}^{(k_1)}$, $\mathbf{i}^{(k_2)}$ and $\mathbf{i}^{(\sum_{K-2})}$ where $\chi = \frac{K}{(K-2)+\rho_{(k_1)}^2+\rho_{(k_2)}^2}$, $\rho_{(k_i)} = \| - (b_1^{(\sum_{K-2})} q_1^{(k_i)} + b_2^{(\sum_{K-2})} q_2^{(k_i)})\|$, $\beta_{(k_i)} = -\frac{1}{\rho_{(k_i)}} (b_1^{(\sum_{K-2})} q_1^{(k_i)} + b_2^{(\sum_{K-2})} q_2^{(k_i)})$ ($i \in \{1,2\}$), CIA-PA can be realized. $b_1^{(k_i)}$, $b_2^{(k_i)}$, $b_1^{(\sum_{K-2})}$, $b_2^{(\sum_{K-2})}$ and $q_i^{(k_i)}$ are complex numbers satisfying $\mathbf{W}_1 \mathbf{i}^{(k_i)} = b_1^{(k_i)} \mathbf{d}_{\mathbf{s}^{(1)}}$, $\mathbf{W}_2 \mathbf{i}^{(k_i)} = b_2^{(k_i)} \mathbf{d}_{\mathbf{s}^{(2)}}$, $\mathbf{W}_1 \mathbf{i}^{(\sum_{K-2})} = b_1^{(\sum_{K-2})} \mathbf{d}_{\mathbf{s}^{(1)}}$, $\mathbf{W}_2 \mathbf{i}^{(\sum_{K-2})} = b_2^{(\sum_{K-2})} \mathbf{d}_{\mathbf{s}^{(2)}}$, $q_1^{(k_1)} = \frac{b_2^{(k_2)}}{b_1^{(k_1)} b_2^{(k_2)} - b_2^{(k_1)} b_1^{(k_2)}}$, $q_1^{(k_2)} = \frac{-b_2^{(k_1)}}{b_1^{(k_1)} b_2^{(k_2)} - b_2^{(k_1)} b_1^{(k_2)}}$, $q_2^{(k_1)} = \frac{b_1^{(k_2)}}{b_1^{(k_2)} b_2^{(k_1)} - b_1^{(k_1)} b_2^{(k_2)}}$ and $q_2^{(k_2)} = \frac{-b_1^{(k_1)}}{b_1^{(k_2)} b_2^{(k_1)} - b_1^{(k_1)} b_2^{(k_2)}}$.

The proof of Lemma 2 is given in Appendix B.

One can see from the proof of Lemma 2 that we have adjusted the interferences under P_T constraint by multiplying each of them by a complex coefficient, so that the orthogonality among the signals at their intended receiver, i.e., STA_1 associated with the interfering AP_1, is guaranteed; moreover, transmission from AP_1 to STA_1 still matches their channel status (see the detailed discussion in Remark 1). Therefore, good performance of the interfering transmission-pair can be achieved.

Remark 1: Given an interference from AP_1 to STA_0, say $\mathbf{i}_1^{(k)}$, whose precoding vector is $\mathbf{p}_1^{(k)}$ obtained by applying singular value decomposition to $\mathbf{H}_{11}$, its corresponding transmission from AP_1 to STA_1 matches $\mathbf{H}_{11}$. Since CIA-PA multiplies a complex coefficient with $\mathbf{i}_1^{(k)}$, without loss of generality, we can use $\zeta_1^{(k)}$ to denote such a coefficient. So, the adjusted interference becomes $\bar{\mathbf{i}}_1^{(k)} = \zeta_1^{(k)} \mathbf{i}_1^{(k)}$. Then, the desired signal perceived at the interfering STA_1, which corresponds to $\bar{\mathbf{i}}_1^{(k)}$, can be expressed as $\bar{\mathbf{s}}_1^{(k)} = \sqrt{\frac{P_T}{K}} \mathbf{H}_{11} \zeta_1^{(k)} \mathbf{p}_1^{(k)} x_1^{(k)}$. We can regard $\zeta_1^{(k)} \mathbf{p}_1^{(k)}$ as a new precoder for the adjusted desired transmission from AP_1 to STA_1. Since $\langle \zeta_1^{(k)} \mathbf{p}_1^{(k)}, \mathbf{d} \rangle = \zeta_1^{(k)} \langle \mathbf{p}_1^{(k)}, \mathbf{d} \rangle$ holds (where $\mathbf{d}$ can be the spatial feature of either a wireless channel or other signal), $\zeta_1^{(k)}$ does not alter the inter-relationship of $\mathbf{p}_1^{(k)}$ and $\mathbf{d}$. Therefore, with CIA-PA, the adjusted transmission from AP_1 to STA_1 still matches the channel status, $\mathbf{H}_{11}$.

The received signals at STA_0 and SAT_1 are given by Eqs. (16)–(17), shown at the bottom of the page. The first term on the right-hand side of Eq. (16) represents the desired signal of STA_0, while the second and third terms are the adjusted interfering signals. The last term is additive white Gaussian noise.

We employ $\mathbf{F}_0 = [\mathbf{f}_0^{(1)} \ \ \mathbf{f}_0^{(2)}]$ and $\mathbf{F}_1 = [\mathbf{f}_1^{(1)} \ \cdots \ \mathbf{f}_1^{(k)} \ \cdots \ \mathbf{f}_1^{(K)}]$ as the filter matrices at STA_0 and STA_1. They can be obtained by applying singular value decomposition to $\mathbf{H}_{00}$ and $\mathbf{H}_{11}$, respectively (see in Section III-A). Then, spectral efficiency of STA_0 and STA_1 can be calculated according to Eqs. (18)–(19) as:

$$c_0^{CIA-PA} = \sum_{g=1}^{2} \log_2 \{1 + \frac{P_T}{2\sigma_n^2} [\lambda_{00}^{(g)}]^2\}, \tag{18}$$

$$c_1^{CIA-PA} = \sum_{i=1}^{2} \log_2 \left\{ 1 + \frac{P_T \chi \rho_{k_i}^2 [\lambda_{11}^{(k_i)}]^2}{K\sigma_n^2} \right\} + \sum_{k=1, k \notin \{k_1, k_2\}}^{K} \log_2 \left\{ 1 + \frac{P_T \chi [\lambda_{11}^{(k)}]^2}{K\sigma_n^2} \right\}. \tag{19}$$

From the design of CIA-SPA and CIA-PA, we can see that the former adjusts one interference's spatial signature and all interferences' strength, whereas the latter only modifies all disturbances' strength. Therefore, CIA-SPA incurs co-channel interference to the interfering transmission-pair while CIA-PA guarantees the orthogonality among all the transmissions from AP_1 to STA_1. However, it should be noted that the application of CIA-PA should satisfy certain conditions. Taking $G = 2$ as an example, when there are only two interfering components to be adjusted with CIA-PA, their projections on $\mathcal{G}$ should have been aligned with each other, so that we can achieve cooperative IA via adjusting the interferences' strength. However, in practice, due to the randomness of wireless channels,

$$\mathbf{y}_0^{CIA-PA} = \sum_{g=1}^{2} \sqrt{\frac{P_T}{2}} \mathbf{H}_{00} \mathbf{p}_0^{(g)} x_0^{(g)} + \sum_{i=1}^{2} \sqrt{\frac{P_T}{K} \chi \rho_{k_i}^2} \beta_{k_i} \mathbf{H}_{10} \mathbf{p}_1^{(k_i)} a_{k_i} x_1^{(\hat{k})} + \sum_{k=1, k \notin \{k_1, k_2\}}^{K} \sqrt{\frac{P_T}{K}} \chi \mathbf{H}_{10} \mathbf{p}_1^{(k)} a_k x_1^{(\hat{k})} + \mathbf{n}_0 \tag{16}$$

$$\mathbf{y}_1^{CIA-PA} = \sum_{i=1}^{2} \sqrt{\frac{P_T}{K} \chi \rho_{k_i}^2} \beta_{k_i} \mathbf{H}_{11} \mathbf{p}_1^{(k_i)} x_1^{(k_i)} + \sum_{k=1, k \notin \{k_1, k_2\}}^{K} \sqrt{\frac{P_T}{K}} \chi \mathbf{H}_{11} \mathbf{p}_1^{(k)} x_1^{(k)} + \mathbf{n}_1 \tag{17}$$

the projections of various interferences on $\mathcal{G}$ are usually not aligned with each other by nature. Therefore, we consider a more common situation as plotted in Fig. 3, showing the existence of at least 3 interferences' projections on $\mathcal{G}$. Then, we can group the disturbances in 3 sets, and for each set we can find a non-zero complex coefficient according to CIA-PA so that the effect of the interferences to $\mathcal{G}$ can be mitigated.

In what follows, we will first present a preliminary based on practical communication, and then give the requirement for realizing CIA-PA in Theorem 1.

Preliminary 1: Due to the randomness of data transmission and wireless channels, the projections of various interferences or the overall effects of groups of interferences on $\mathcal{G}$ are always different/non-aligned.[2]

Theorem 1: Given K interferences, G desired signals of the interfered transmitter–receiver pair, and K interferences are grouped in D sets. We define an effective interference matrix as $\mathcal{I} = [\mathbf{i}_e^{(1)} \ \cdots \ \mathbf{i}_e^{(d)} \ \cdots \ \mathbf{i}_e^{(D)}]$, where $\mathbf{i}_e^{(d)}$ denotes the projection of the overall effect of disturbances in group d on the desired signal subspace $\mathcal{G}$. CIA-PA is applicable if rank$(\mathcal{I}) < D$.

The proof is given in Appendix C.

In addition to the above theorem, we can have Lemma 3 as:

Lemma 3: Given K interferences and that the rank of the desired signals subspace is G, CIA-PA can be applied as long as $D \geq G + 1$.

The proof is given in Appendix D. Note that Lemma 3 shows the sufficient (but unnecessary) condition for the availability of CIA-PA. That is, based on the proof of Lemma 3, rank$(\mathcal{I}) < D$ can be derived from $D \geq G + 1$, and then according to Theorem 1, CIA-PA is applicable. However, given $D < G + 1$, relations between rank$(\mathcal{I})$ and D cannot be determined. In such a case, we need to check the condition of rank$(\mathcal{I}) < D$ given in Theorem 1 so as to determine the feasibility of CIA-PA.

According to Theorem 1 and Lemma 3, given desired signals subspace $\mathcal{G}$, we should divide K interferences into $D \leq G + 1$ groups. Then, under rank$(\mathcal{I}) = D - 1$, we can employ CIA-PA. Under such a condition, we can obtain D power coefficients of which at least one is non-zero. As for those interferences with zero power coefficient, their corresponding data transmissions are turned off.

Note that in the existing design of CIA-PA, we assume two of the three interference sets contain only one disturbance. In practice, the interference set can have an arbitrary number of disturbances. However, since we can treat the overall effect of multiple interfering components in a set as an effective interference, the group involving multiple interferences can be equivalent to that containing a single interference. So, the proposed methods can be directly applied.

So far, we have detailed the design of cooperative IA in managing multiple interferences from the same source. This situation is more difficult than that contains disturbances from different sources [19]. However, our scheme can be readily applied to the case of involving multiple interferers and each interferer generating multiple interferences, as analyzed below. On one hand, each interfering source can carry out cooperative IA independently so as to achieve alignment of its own interferences at the interfered receiver. On the other hand, multiple interferers can cooperate with each other in implementing cooperative IA. As for the cooperative case, multiple interfering sources can be treated as one virtual source, causing interferences to a receiver. Then, CIA-SPA/PA can be readily applied. It should be noted that in the use of CIA-PA, the interferences adjusted in the first phase can be either from the same source or different sources.

[2]The spatial features of the projections are not aligned in the same one-dimensional subspace, e.g., as shown in Fig. 3 vectors $\mathbf{i}_e^{(k_1)}$, $\mathbf{i}_e^{(k_2)}$ and $\mathbf{i}_e^{(\Sigma_{K-2})}$ are in various/different directions.

IV. Evaluation

We use MATLAB simulation to demonstrate the advantages of the proposed cooperative IA schemes over others. We consider two APs and two STAs. AP_0 and STA_0 constitute the interfered transmission-pair, while AP_1 and STA_1 form an interfering transmission-pair. Transmit power of each AP is P_T. Since cooperative IA exploits interactions among multiple interfering signals and manages their overall effect, instead of each individual effect, only one DoF is required for placing the aligned interferences. That is, as long as the number of desired signals of the interfered STA is less than N_R, cooperative IA is applicable. So, the feasibility of cooperative IA is independent of the relation between N_T and N_R. Even when $N_T < N_R$, the proposed schemes are still applicable; in such a case, as a larger N_R provides more DoFs at the interfered receiver-side, cooperative IA's application can be facilitated. However, since the main advantage of cooperative IA over traditional IA lies in the fact that cooperative IA is feasible under a stringent receiver-side DoF constraint (as small as one DoF cost for interference management) while IA is inapplicable in such situation, and $N_T \geq N_R$ is also common in practical downlink transmissions, we omit the discussion and evaluation of the case of $N_T < N_R$. For simplicity, we set $N_T = N_R = \overline{N}$. We define the signal-to-noise ratio as $\gamma = 10\log_{10}\frac{P_T}{\sigma_n^2}$dB, and set $\gamma \in [0, 20]$dB. Besides the proposed CIA-SPA and CIA-PA, we also simulated interference neutralization (IN) [4], single target interference steering (STIS), aggregated interference steering (AIS) [7] and non-interference-management (non-IM) for comparison. As for non-IM, the interfered receiver employs matched filtering to decode its desired data while leaving the interference un-managed.

Fig. 4 plots the average system SE, i.e., the sum spectral efficiency of both interfered and interfering transmission-pairs, under $N_T = N_R = 4$ and different γs. The numbers of interfered transmissions and interferences are $G = 3$ and $K = 4$, respectively. In such parameter settings, there is only one DoF at the interfered receiver available for interference management. So, zero-forcing reception [3], zero-forcing beamforming [8], conventional IA [11]–[14], as well as its evolution [15], [18], are inapplicable. Since cooperative IA is interfering transmitter-side realization (in such a case, the interfered transmission becomes an ideal point-to-point MIMO communication) whereas IS (including AIS and STIS) and IN are interfered transmitter-side implementation (in this case, the interfering transmission is an ideal point-to-point MIMO communication), we study their system SE.

With CIA-SPA, we can either randomly/arbitrarily select the interference indexed by k^* ($k^* \in \{1, 2, \cdots, K\}$) to adjust its spatial signature, yielding system spectral efficiency denoted by *CIA-SPA$_{Rand}$*, or select the disturbance yielding the maximum system spectral efficiency represented by *CIA-SPA$_{Opt}$*. We obtain CIA-SPA$_{\text{Opt}}$ via an exhaustive search. Specifically, we select each of the K interferences as $\mathbf{i}^{(k^*)}$, and then adjust the disturbances according to CIA-SPA and compute the corresponding system SE, so that we can obtain the maximum system spectral efficiency out of the K calculated spectral efficiency values. Similarly, under CIA-PA, K interferences are randomly divided into $D = G + 1$ groups according to Lemma 3, then interference groups for the first-phase adjustment can be arbitrarily selected, this realization is denoted as *CIA-PA$_{Rand}$*. We can also find the best way to group the disturbances and adjust their power so as to achieve the maximum system SE, implementation of which is called *CIA-PA$_{Opt}$*. As for CIA-PA$_{\text{Opt}}$, exhaustive search is applied to all possible interference grouping and power adjustment solutions. We first divide K interferences into $D = G + 1$ groups according to Lemma 3 to ensure that CIA-PA is applicable, and there will be various grouping results. Then, we apply CIA-PA to each grouping result, yielding multiple power adjustment strategies. We can calculate system spectral efficiency for each of the grouping and power adjustment strategies, and then select the one yielding the maximum SE. For example, when $G = 2$ and $K = 4$, we adopt $D = G+1 = 3$ interference sets, so that the numbers of interfering components in the 3 sets are 1, 1, and 2, respectively, there are $\frac{1}{2}C_4^1 C_3^1 C_2^2 = 6$ different grouping results; as for each grouping result, one interference set is selected out of the three and then the projection of interference or the overall effect of all interferences in the selected set on the desired signal subspace is represented by those of interferences in the other two sets, as shown in Eq. (27), to realize CIA-PA, yielding $C_3^1 = 3$ different power adjustment strategies. As a result, there are 18 possible grouping and power adjusting modes in total under $G = 2$ and $K = 4$. For each of the 18 modes, we compute the system SE, and then get the maximum system spectral efficiency out of the calculated spectral efficiency values. Based on the above discussion, under the parameter settings of Fig. 4, i.e., $G = 3$ and $K = 4$, interferences are divided in $D = 4$ groups, and then CIA-PA$_{\text{Opt}}$ is obtained by exhaustive search over 4 grouping and power adjusting modes. With non-IM, precoders and receive filters of interfering and interfered transmission-pairs are determined by employing singular value decomposition based pre- and post-processing (as discussed in Section III), while leaving the interferences without management. Therefore, non-IM can be used as a base line in the evaluation of the proposed cooperative IA schemes.

As Fig. 4 shows, CIA-SPA$_{\text{Opt}}$ and CIA-PA$_{\text{Opt}}$ outperform CIA-SPA$_{\text{Rand}}$ and CIA-PA$_{\text{Rand}}$, respectively, in system SE. Since CIA-PA achieves alignment of interferences at the interfered receiver via power adjustment, it can maintain the orthogonality among multiple transmissions from interfering transmitter to its intended receiver. So, CIA-PA outperforms CIA-SPA. When γ is small, spectral efficiency of CIA-SPA$_{\text{Opt}}$ is higher than that of AIS. This is because at low γ, noise dominates the system SE. The performance loss incurred by the power cost for AIS is severer than that caused by the co-channel interference produced with CIA-SPA. When γ is high, AIS outperforms CIA-SPA$_{\text{Opt}}$. This is because as γ grows, interference becomes the main factor affecting the system SE. In such a situation, co-channel interference incurred by CIA-SPA disrupts the interfering transmission-pair's performance more than the power cost for AIS does. As for IN, since multiple neutralizing signals are generated to mitigate K interferences separately, more power cost than AIS and STIS is incurred. Therefore, the feasibility of IN is low [5]. In our simulation, when an interference management method is inapplicable, we simply switch to non-IM. So, spectral efficiency of IN overlaps with that of non-IM.

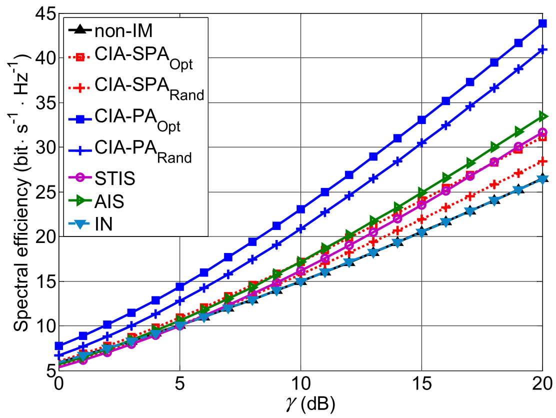

Fig. 4. Comparison of system spectral efficiency with various methods.

In Fig. 5 we compares the proposed cooperative IA schemes with non-IM under $\overline{N} = 4$, $G = 3$, $K \in \{2, 3, 4\}$ and various γs. For clarity, we employ a general form $[K, G]$ to indicate the parameter settings. In addition, we define $\Delta_{SE}^{\mathcal{M}} = \sum_{i=0}^{1} c_i^{\mathcal{M}} - \sum_{i=0}^{1} c_i^{non-IM}$ as the spectral efficiency difference of method $\mathcal{M}$ and non-IM, so that one can easily grasp the performance gain of interference management method $\mathcal{M}$ over the non-IM mode under certain parameter settings. $c_i^{\mathcal{M}}$ and c_i^{non-IM} denote the spectral efficiency of transmission-pair i with method $\mathcal{M}$ and non-IM, respectively. $\mathcal{M}$ can be either CIA-SPA/PA$_{\text{Opt}}$ or CIA-SPA/PA$_{\text{Rand}}$. As Fig. 5(a) shows, given the same G, spectral efficiency of CIA-SPA$_{\text{Opt}}$ grows with an increase of K when γ is high. This is because 1) the larger K the more selective diversity gain, and hence CIA-SPA$_{\text{Opt}}$ can output higher spectral efficiency under larger K; and 2) when γ is large interference dominates the system SE, thus interference management is more beneficial to SE. Therefore, given high γ, system spectral efficiency increases as K grows. When γ is low, noise is the main factor affecting the system SE, therefore, spectral efficiency loss of the interfering transmission-pair incurred by the introduced co-channel interference can outweigh the spectral efficiency improvement of the interfered transmission-pair with interference management. So, in low γ region, CIA-SPA$_{\text{Opt}}$ outputs similar (when $K \in \{3, 4\}$) or even worse (under $K = 2$)

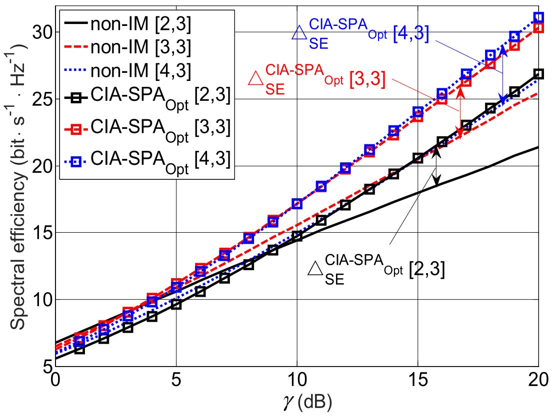

(a) CIA-SPA$_{\mathrm{Opt}}$.

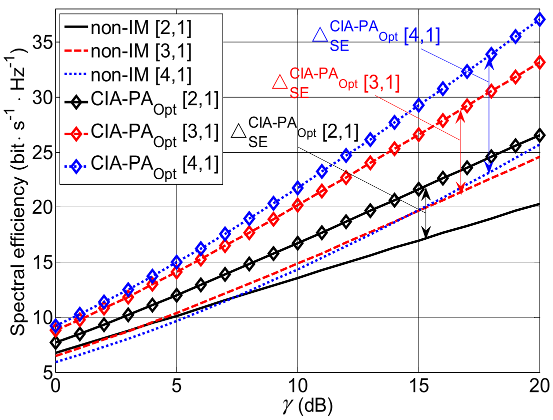

(b) CIA-PA$_{\mathrm{Opt}}$.

Fig. 5. System spectral efficiency of cooperative IA schemes under various K and G.

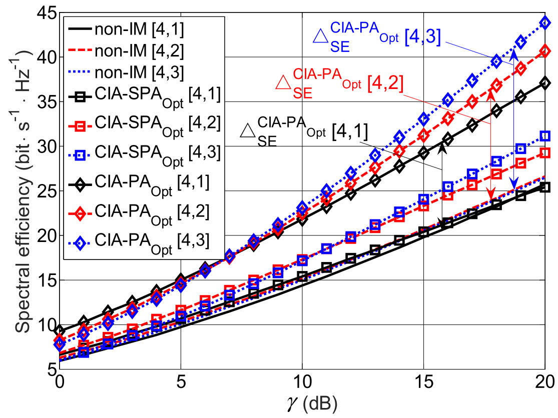

(a) CIA-SPA/PA$_{\mathrm{Opt}}$ vs. non-IM.

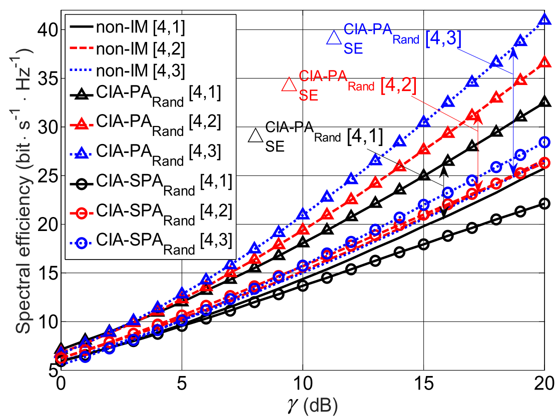

(b) CIA-SPA/PA$_{\mathrm{Rand}}$ vs. non-IM.

Fig. 6. Comparison of cooperative IA schemes and non-IM under $K = 4$ and various G.

spectral efficiency performance than non-IM. Given medium to high γ, $\Delta_{SE}^{CIA-SPA_{Opt}}$ grows with an increase of K.

Fig. 5(b) plots the average system spectral efficiency of CIA-PA$_{\mathrm{Opt}}$ and non-IM under $\overline{N} = 4$, $G = 1$ and $K \in \{2, 3, 4\}$. In this experiment we set $G = 1$ and analyzed the results as follows. According to Lemma 3, setting $D = G+1$ can guarantee the feasibility of CIA-PA, and hence we adopt $D = G + 1$ in the simulation. Moreover, since D is also restricted by K, we set $G = 1$ under $K \in \{2, 3, 4\}$ so that $D = G + 1$ is satisfied. As Fig. 5(b) shows, given the same G, system spectral efficiency of CIA-PA$_{\mathrm{Opt}}$ grows with the increase of K. This is because the number of candidate solutions which reflects the selective diversity gain of CIA-PA, increases as K grows, so that CIA-PA$_{\mathrm{Opt}}$ can output higher system spectral efficiency under a larger K. Moreover, $\Delta_{SE}^{CIA-PA_{Opt}}$ grows as K increases.

Fig. 6 plots the average system spectral efficiency of various CIA-PA realizations and non-IM under $\overline{N} = 4$, $K = 4$ and $G \in \{1, 2, 3\}$. As Fig. 6(a) shows, since CIA-PA$_{\mathrm{Opt}}$ achieves IA without introducing co-channel interference, it outperforms the other two schemes. Given fixed K, system spectral efficiency of both CIA-SPA$_{\mathrm{Opt}}$ and CIA-PA$_{\mathrm{Opt}}$ grows with an increase of G at high SNR. This is because spectral efficiency of the interfered transmission-pair employing spatial multiplexing (SM) improves at high γ [3], so that the benefits brought by both cooperative IA schemes to the system spectral efficiency increase as G grows. Moreover, $\Delta_{SE}^{CIA-PA_{Opt}}$ grows with an increase of G.

In Fig. 6(b), spectral efficiency of CIA-SPA/PA$_{\mathrm{Rand}}$ is simulated. Note that under $G = 1$, spectral efficiency of CIA-SPA$_{\mathrm{Rand}}$ is lower than that of non-IM. This is because CIA-SPA incurs co-channel interference to the interfering transmission-pair, hence decreasing its SE. Moreover, this spectral efficiency reduction outweighs the limited increase of spectral efficiency that CIA-SPA$_{\mathrm{Rand}}$ brings to the interfered transmission-pair consisting $G = 1$ desired signal. So, system spectral efficiency decreases under $G = 1$. As the figure shows, $\Delta_{SE}^{CIA-PA_{Rand}}$ grows as G increases.

Fig. 7 exhibits the system average spectral efficiency of CIA-SPA/PA$_{\mathrm{Opt}}$, AIS and non-IM under $\overline{N}$, $K = \overline{N}$ and $G = \overline{N} - 1$. $\overline{N} \in \{2, 4, 6\}$ and $\overline{N} \in \{2, 3, 4\}$ are adopted in two subplots, respectively. We adopt a general form $[K, G, \overline{N}]$ to denote the parameter settings. As Fig. 7(a) shows, spectral efficiency of all schemes increases with an increase of $\overline{N}$. CIA-SPA$_{\mathrm{Opt}}$ excels non-IM and AIS in system spectral efficiency under a large $\overline{N}$ while is inferior to AIS when $\overline{N}$ is small. Moreover, $\Delta_{SE}^{CIA-SPA_{Opt}}$ gradually enlarges as $\overline{N}$, and accordingly G and K, increase. This is analyzed as follows. Under non-IM, spectral efficiency of

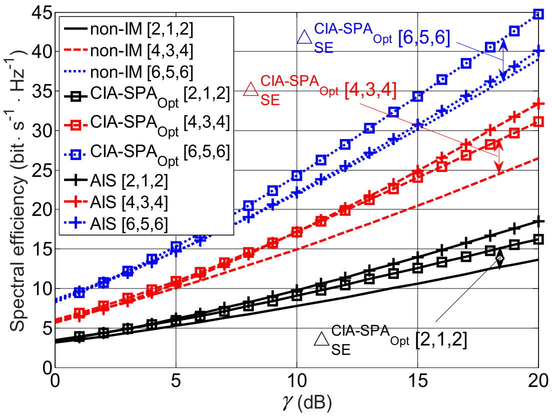

(a) CIA-SPA$_{\text{Opt}}$ vs. AIS and non-IM.

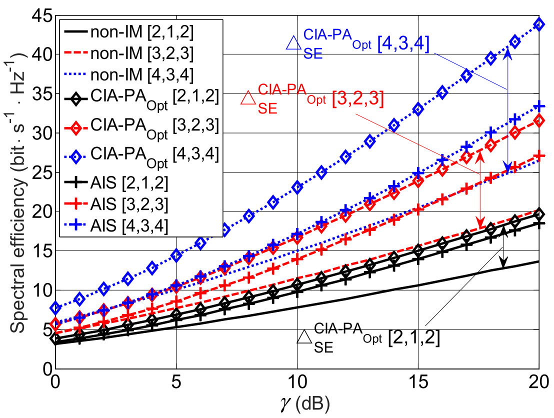

(b) CIA-PA$_{\text{Opt}}$ vs. AIS and non-IM.

Fig. 7. Comparison of cooperative IA and other schemes under various $\overline{N}$, K and G.

both interfering and interfered transmission-pairs grows as $\overline{N}$ increases due to the SM gain, even though the interfered transmission-pair's spectral efficiency saturates as γ grows [7], the system spectral efficiency still improves with an increase of $\overline{N}$. As for AIS, on one hand, spectral efficiency of the interfering transmission-pair which is free of disturbance with interference management, increases as $\overline{N}$ grows; on the other hand, as for the interfered transmission-pair, the number of projecting components of an interference on each desired transmission grows as G increases, incurring more power cost for AIS and hence more spectral efficiency loss. When the power overhead of AIS exceeds P_T at AP$_0$, AIS becomes unavailable and is switched to non-IM. Therefore, when $\overline{N}$ is large, yielding big G and K, AIS is slightly better than non-IM. With CIA-SPA$_{\text{Opt}}$, no transmit power is consumed for interference management unlike AIS. Moreover, spectral efficiency of CIA-SPA$_{\text{Opt}}$ can benefit from the array processing gain brought by multiple antennas employed on both sides of the communication link.

Fig. 7(b) compares CIA-PA$_{\text{Opt}}$ with AIS and non-IM under $\overline{N} \in \{2, 3, 4\}$, $K = \overline{N}$ and $G = \overline{N} - 1$. Spectral efficiency of all schemes is shown to grow with an increase of $\overline{N}$. Since CIA-PA$_{\text{Opt}}$ achieves multi-interference alignment without introducing co-channel interference, it can significantly improve system spectral efficiency over the other two schemes.

V. Conclusion

In this paper, we have proposed two cooperative IA schemes, CIA-SPA and CIA-PA, to manage multiple interferences. By exploiting interactions among multiple wireless disturbances, cooperative IA aligns the overall effect of all interferences in the orthogonal direction with respect to the desired transmission(s) at the interfered receiver. CIA-SPA modifies one interference's spatial signature and all interferences' strength, while CIA-PA adjusts all interfering signals' strength. Compared to the conventional IA, at most one interference spatial feature is modified, so that the orthogonality of the interfering transmission-pair's signals can be preserved as much as possible, and hence less (CIA-SPA) or no co-channel interference (CIA-PA) is incurred. In addition, the proposed schemes can be applied to the situations where multiple interferences are from either identical or different sources. Our theoretical analysis and in-depth simulation results have shown that the proposed schemes can effectively manage multiple interferences while achieving good system spectral efficiency.

Appendix A
Proof of Lemma 1

Eq. (6) can be simplified as:

$$\mathbf{W}_{\mathcal{G}}\mathbf{H}_{10}\sqrt{\frac{\varepsilon_{k^*}}{\varepsilon_k}}\overline{\mathbf{p}}_1^{(k^*)}a_{k^*} = -\mathbf{W}_{\mathcal{G}}\mathbf{H}_{10}\sum_{k=1,k\neq k^*}^{K}\mathbf{p}_1^{(k)}a_k. \quad (20)$$

Then, we adopt:

$$\sqrt{\frac{\varepsilon_{k^*}}{\varepsilon_k}}\overline{\mathbf{p}}_1^{(k^*)} = -(\mathbf{W}_{\mathcal{G}}\mathbf{H}_{10}a_{k^*})^{\dagger}\mathbf{W}_{\mathcal{G}}\mathbf{H}_{10}\sum_{k=1,k\neq k^*}^{K}\mathbf{p}_1^{(k)}a_k \quad (21)$$

and substitute it into the left-hand side of Eq. (20) to acquire Eq. (22) as below.

By exploiting the fact that given a matrix $\mathbf{A} \in \mathbb{C}^{m\times n}$, its pseudo inverse $\mathbf{A}^{\dagger}$ exclusively exists and $\mathbf{A}\mathbf{A}^{\dagger}\mathbf{A} = \mathbf{A}$ holds [27], we can prove that Eq. (21) satisfies Eq. (20). Since the parameters on the right-hand side of Eq. (21) are known, we can have the expression of $\overline{\mathbf{p}}_1^{(k^*)}$, i.e., Eq. (7), where $r = \|-(\mathbf{W}_{\mathcal{G}}\mathbf{H}_{10}a_{k^*})^{\dagger}\mathbf{W}_{\mathcal{G}}\mathbf{H}_{10}\sum_{k=1,k\neq k^*}^{K}\mathbf{p}_1^{(k)}a_k\| = \sqrt{\frac{\varepsilon_{k^*}}{\varepsilon_k}}$. Recall that the transmit power of the K interferences satisfies $\frac{P_T}{K}\varepsilon_{k^*} + (K-1)\frac{P_T}{K}\varepsilon_k = P_T$ from which we can have $\varepsilon_k = \frac{K-\varepsilon_{k^*}}{K-1}$, and then obtain an equation set as:

$$\begin{cases}\varepsilon_k = \frac{K-\varepsilon_{k^*}}{K-1}\\ \sqrt{\varepsilon_{k^*}/\varepsilon_k} = r.\end{cases} \quad (23)$$

$$\mathbf{W}_{\mathcal{G}}\mathbf{H}_{10}a_{k^*}\sqrt{\frac{\varepsilon_{k^*}}{\varepsilon_k}}\overline{\mathbf{p}}_1^{(k^*)} = -(\mathbf{W}_{\mathcal{G}}\mathbf{H}_{10}a_{k^*})(\mathbf{W}_{\mathcal{G}}\mathbf{H}_{10}a_{k^*})^{\dagger}(\mathbf{W}_{\mathcal{G}}\mathbf{H}_{10}a_{k^*})\frac{1}{a_{k^*}}\sum_{k=1,k\neq k^*}^{K}\mathbf{p}_1^{(k)}a_k. \quad (22)$$

Substituting $\varepsilon_{k^*} = r^2\varepsilon_k$ and $\varepsilon_k = r^{-2}\varepsilon_k^*$, respectively, into the first equation of Eq. (23), we can solve the power coefficients set as given in Eqs. (8)–(9). Therefore, Lemma 1 follows. ■

APPENDIX B
PROOF OF LEMMA 2

Since $\mathbf{W}_1$ and $\mathbf{W}_2$ are projection matrices with respect to $\mathbf{d}_{\mathbf{s}^{(1)}}$ and $\mathbf{d}_{\mathbf{s}^{(2)}}$, respectively, we can use equations $\mathbf{W}_1\mathbf{i}^{(k_1)} = b_1^{(k_1)}\mathbf{d}_{\mathbf{s}^{(1)}}$, $\mathbf{W}_2\mathbf{i}^{(k_1)} = b_2^{(k_1)}\mathbf{d}_{\mathbf{s}^{(2)}}$, $\mathbf{W}_1\mathbf{i}^{(k_2)} = b_1^{(k_2)}\mathbf{d}_{\mathbf{s}^{(1)}}$, $\mathbf{W}_2\mathbf{i}^{(k_2)} = b_2^{(k_2)}\mathbf{d}_{\mathbf{s}^{(2)}}$, $\mathbf{W}_1\mathbf{i}^{(\sum_{K-2})} = b_1^{(\sum_{K-2})}\mathbf{d}_{\mathbf{s}^{(1)}}$ and $\mathbf{W}_2\mathbf{i}^{(\sum_{K-2})} = b_2^{(\sum_{K-2})}\mathbf{d}_{\mathbf{s}^{(2)}}$ where $b_1^{(k_1)}$, $b_2^{(k_1)}$, $b_1^{(k_2)}$, $b_2^{(k_2)}$, $b_1^{(\sum_{K-2})}$ and $b_2^{(\sum_{K-2})}$ are complex numbers, to rewrite Eqs. (14)–(15) as:

$$\mathbf{i}_e^{(k_i)} = b_1^{(k_i)}\mathbf{d}_{\mathbf{s}^{(1)}} + b_2^{(k_i)}\mathbf{d}_{\mathbf{s}^{(2)}} \tag{24}$$

$$\mathbf{i}_e^{(\sum_{K-2})} = b_1^{(\sum_{K-2})}\mathbf{d}_{\mathbf{s}^{(1)}} + b_2^{(\sum_{K-2})}\mathbf{d}_{\mathbf{s}^{(2)}}. \tag{25}$$

By substituting k_1 and k_2 into Eq. (24), respectively, we can get an equation set containing two equations. Then, we can have:

$$\mathbf{d}_{\mathbf{s}^{(i)}} = q_i^{(k_1)}\mathbf{i}_e^{(k_1)} + q_i^{(k_2)}\mathbf{i}_e^{(k_2)} \tag{26}$$

where $i \in \{1,2\}$, $q_i^{(k_1)}$ and $q_i^{(k_2)}$ are complex coefficients satisfying $q_1^{(k_1)} = \frac{b_2^{(k_2)}}{b_1^{(k_1)}b_2^{(k_2)} - b_2^{(k_1)}b_1^{(k_2)}}$, $q_1^{(k_2)} = \frac{-b_2^{(k_1)}}{b_1^{(k_1)}b_2^{(k_2)} - b_2^{(k_1)}b_1^{(k_2)}}$, $q_2^{(k_1)} = \frac{b_1^{(k_2)}}{b_1^{(k_2)}b_2^{(k_1)} - b_1^{(k_1)}b_2^{(k_2)}}$ and $q_2^{(k_2)} = \frac{-b_1^{(k_1)}}{b_1^{(k_2)}b_2^{(k_1)} - b_1^{(k_1)}b_2^{(k_2)}}$.

From Eqs. (25)–(26), we have:

$$\mathbf{i}_e^{(\sum_{K-2})} = (b_1^{(\sum_{K-2})}q_1^{(k_1)} + b_2^{(\sum_{K-2})}q_2^{(k_1)})\mathbf{i}_e^{(k_1)} + (b_1^{(\sum_{K-2})}q_1^{(k_2)} + b_2^{(\sum_{K-2})}q_2^{(k_2)})\mathbf{i}_e^{(k_2)}. \tag{27}$$

We let $\bar{\mathbf{i}}_e^{(\sum_{K-2})} = \mathbf{i}_e^{(\sum_{K-2})}$, $\bar{\mathbf{i}}_e^{(k_1)} = -(b_1^{(\sum_{K-2})}q_1^{(k_1)} + b_2^{(\sum_{K-2})}q_2^{(k_1)})\mathbf{i}_e^{(k_1)}$, and $\bar{\mathbf{i}}_e^{(k_2)} = -(b_1^{(\sum_{K-2})}q_1^{(k_2)} + b_2^{(\sum_{K-2})}q_2^{(k_2)})\mathbf{i}_e^{(k_2)}$, i.e., only $\mathbf{i}^{(k_1)}$ and $\mathbf{i}^{(k_2)}$ are adjusted in the first phase. Then, $\sum_{i=1}^{2}\bar{\mathbf{i}}_e^{(k_i)} + \bar{\mathbf{i}}_e^{(\sum_{K-2})} = \mathbf{0}$ holds.

From the above discussion one can see that the first-phase adjustment can mitigate the effect of the interferences to the desired transmission at the interfered receiver. However, since we introduce complex coefficients $-(b_1^{(\sum_{K-2})}q_1^{(k_1)} + b_2^{(\sum_{K-2})}q_2^{(k_1)})$ and $-(b_1^{(\sum_{K-2})}q_1^{(k_2)} + b_2^{(\sum_{K-2})}q_2^{(k_2)})$ to modify $\mathbf{i}^{(k_1)}$ and $\mathbf{i}^{(k_2)}$, and their effective part on $\mathcal{G}$, $\mathbf{i}_e^{(k_1)}$ and $\mathbf{i}_e^{(k_2)}$ change accordingly, the total power constraint at the interfering transmitter may not hold. Therefore, we need to make the second-phase adjustment to satisfy the transmit power constraint, P_T, at AP_1. We define $\rho_{(k_i)} = \| -(b_1^{(\sum_{K-2})}q_1^{(k_i)} + b_2^{(\sum_{K-2})}q_2^{(k_i)})\|$ and $\beta_{(k_i)} = -\frac{1}{\rho_{(k_i)}}(b_1^{(\sum_{K-2})}q_1^{(k_i)} + b_2^{(\sum_{K-2})}q_2^{(k_i)})$. $\|\beta_{(k_i)}\| = 1$ holds. Then, we can have the coefficient for CIA-PA in the first phase as $\rho_{(k_i)}\beta_{(k_i)}$ where $i \in \{1,2\}$.

In the second phase, since the transmit power of AP_1 cannot exceed P_T, Eq. (28) should hold as follows:

$$\chi\left\{\frac{P_T}{K}(K-2) + \frac{P_T}{K}\rho_{(k_1)}^2 + \frac{P_T}{K}\rho_{(k_2)}^2\right\} = P_T \tag{28}$$

where $\chi \in (0, \frac{K}{K-2})$ is a new coefficient introduced in the second phase for proportionally adjusting all the interferences modified in the first phase. From Eq. (28) we can obtain:

$$\chi = \frac{K}{(K-2) + \rho_{(k_1)}^2 + \rho_{(k_2)}^2}. \tag{29}$$

Finally, we can have the coefficients $\sqrt{\chi\rho_{(k_1)}^2}\beta_{(k_1)}$, $\sqrt{\chi\rho_{(k_2)}^2}\beta_{(k_2)}$ and $\sqrt{\chi}$ for adjusting $\mathbf{i}^{(k_1)}$, $\mathbf{i}^{(k_2)}$ and $\mathbf{i}^{(\sum_{K-2})}$. Therefore, Lemma 2 follows. ■

APPENDIX C
PROOF OF THEOREM 1

First, we verify CIA-PA's feasibility under $\mathrm{rank}(\mathcal{I}) = D-1$. As is known, if vectors $\mathbf{a}_1, \mathbf{a}_2, \cdots, \mathbf{a}_L$ are linearly independent, while their extension $\mathbf{a}_1, \mathbf{a}_2, \cdots, \mathbf{a}_L, \mathbf{b}$ are linearly dependent, then $\mathbf{b}$ can be linearly and exclusively represented by $\mathbf{a}_1, \mathbf{a}_2, \cdots, \mathbf{a}_L$ [27]. Given K interferences, we divide them into D groups to obtain $\mathcal{I} = [\mathbf{i}_e^{(1)} \cdots \mathbf{i}_e^{(d)} \cdots \mathbf{i}_e^{(D)}]$ where $\mathbf{i}_e^{(d)}$ denotes the projection of the overall effect of interference(s) in group index by d on the desired signal subspace $\mathcal{G}$. When $\mathrm{rank}(\mathcal{I}) = D-1$, there exist $D-1$ linearly independent vectors in $\mathcal{I}$. Without loss of generality, we let the remaining vector other than the $D-1$ linearly independent ones, be $\mathbf{i}_e^{(d^*)}$, then we can have:

$$\mathbf{i}_e^{(d^*)} = \sum_{d\in\{1,\cdots,D\}\backslash\{d^*\}} h_d\mathbf{i}_e^{(d)} \tag{30}$$

where $h_d \in \mathbb{C}$ and $d \in \{1,\cdots,D\}\backslash\{d^*\}$. Eq. (30) indicates that $\mathbf{i}_e^{(d^*)}$ can be expressed by the linear combination of the $D-1$ independent vectors.

We can rewrite Eq. (30) as $\mathbf{i}_e^{(d^*)} + \sum_{d\in\{1,\cdots,D\}\backslash\{d^*\}}(-h_d)\mathbf{i}_e^{(d)} = \mathbf{0}$, from which we find that multiplying each $\mathbf{i}_e^{(d)}$ with a complex coefficient $-h_d$, the sum effect of $D-1$ interferences can counteract $\mathbf{i}_e^{(d^*)}$, thus yielding no effective disturbance to the desired transmission. So, power adjustment in phase-one is done. Then, in phase-two, we need to further adjust all interferences' transmit power in proportion to their strength in the end of phase-one, so that the power constraint P_T at the interfering transmitter is satisfied. Based on the above analysis, CIA-PA is applicable under $\mathrm{rank}(\mathcal{I}) = D-1$.

Next, we analyze the validity of CIA-PA under $\mathrm{rank}(\mathcal{I}) = D$ and $\mathrm{rank}(\mathcal{I}) < D-1$, respectively, as follows. Given $\mathrm{rank}(\mathcal{I}) = D$, there are D independent vectors in $\mathcal{I}$. So, we cannot find a vector in $\mathcal{I}$, say $\mathbf{i}_e^{(d^*)}$, to be expressed by a linear combination of the D vectors in $\mathcal{I}$. That is, we cannot find a set of h_ds satisfying $\mathbf{i}_e^{(d^*)} + \sum_{d\in\{1,\cdots,D\}\backslash\{d^*\}}(-h_d)\mathbf{i}_e^{(d)} = \mathbf{0}$. Therefore, CIA-PA is inapplicable under $\mathrm{rank}(\mathcal{I}) = D$.

When $\mathrm{rank}(\mathcal{I}) < D-1$, we first discuss the case of $\mathrm{rank}(\mathcal{I}) = D-2$. Similarly to the previous discussion, $\mathrm{rank}(\mathcal{I}) = D-2$ means that $D-2$ linearly independent vectors exist in matrix $\mathcal{I}$. Then, we use $\mathbf{i}_e^{(d_1^*)}$ and $\mathbf{i}_e^{(d_2^*)}$ to denote the remaining two vectors in $\mathcal{I}$, and can have:

$$\mathbf{i}_e^{(d_1^*)} = \sum_{d\in\{1,\cdots,D\}\backslash\{d_1^*,d_2^*\}} h_d^{(d_1^*)}\mathbf{i}_e^{(d)} \tag{31}$$

and

$$\mathbf{i}_e^{(d_2^*)} = \sum_{d\in\{1,\cdots,D\}\backslash\{d_1^*,d_2^*\}} h_d^{(d_2^*)} \mathbf{i}_e^{(d)}. \tag{32}$$

That is, $\mathbf{i}_e^{(d_1^*)}$ and $\mathbf{i}_e^{(d_2^*)}$ can be expressed as a linear combination of the $D-2$ independent elements in $\mathcal{I}$. $\{h_d^{(d_1^*)}\}$ and $\{h_d^{(d_2^*)}\}$ denote two complex coefficient sets corresponding to the expressions of $\mathbf{i}_e^{(d_1^*)}$ and $\mathbf{i}_e^{(d_2^*)}$, respectively. Then, for simplicity, we can group $\mathbf{i}_e^{(d_1^*)}$ and $\mathbf{i}_e^{(d_2^*)}$ in one set so that the overall effect of $\mathbf{i}_e^{(d_1^*)}$ and $\mathbf{i}_e^{(d_2^*)}$ in the same group can be expressed as a linear combination of the $D-2$ independent elements in $\mathcal{I}$ with coefficients set $\{h_d^{(d_1^*)}+h_d^{(d_2^*)}\}$, i.e., $\mathbf{i}_e^{(d_1^*)}+\mathbf{i}_e^{(d_2^*)}+\sum_{d\in\{1,\cdots,D\}\backslash\{d_1^*,d_2^*\}}(-h_d^{(d_1^*)}-h_d^{(d_2^*)})\mathbf{i}_e^{(d)}=\mathbf{0}$ holds and the sum effect of $D-2$ interferences counteracts $\mathbf{i}_e^{(d_1^*)}+\mathbf{i}_e^{(d_2^*)}$. In other words, by grouping $\mathbf{i}_e^{(d_1^*)}$ and $\mathbf{i}_e^{(d_2^*)}$ in one set, the number of interference groups reduces to $D'=D-1$, yielding a new effective interference matrix $\mathcal{I}'=[\mathbf{i}_e^{(1)}\ \cdots\ \mathbf{i}_e^{(d)}\ \cdots\ \mathbf{i}_e^{(D')}]$ satisfying $\text{rank}(\mathcal{I}')=D'-1$, so that CIA-PA is available.

Similarly to the above analysis under $\text{rank}(\mathcal{I})=D-2$, as for $\text{rank}(\mathcal{I})<D-2$, there exist $\text{rank}(\mathcal{I})$ linearly independent vectors in $\mathcal{I}$. By grouping the remaining $D-\text{rank}(\mathcal{I})$ vectors of $\mathcal{I}$ in one set, the number of groups becomes $D'=\text{rank}(\mathcal{I})+1$, yielding matrix $\mathcal{I}'=[\mathbf{i}_e^{(1)}\ \cdots\ \mathbf{i}_e^{(d)}\ \cdots\ \mathbf{i}_e^{(D')}]$. Since $\text{rank}(\mathcal{I}')=D'-1$, CIA-PA is applicable to D' groups of interferences.

Therefore, based on the above discussion, Theorem 1 follows. ■

Appendix D
Proof of Lemma 3

As is known, the necessary and sufficient condition for the linear dependence of a set of vectors $\mathbf{a}_1$, $\mathbf{a}_2$, $\cdots$, $\mathbf{a}_L$ is $\text{rank}(\mathbf{A})<L$ where $\mathbf{A}=[\mathbf{a}_1\ \cdots\ \mathbf{a}_L]$; and the necessary and sufficient condition for the linear independence of $\mathbf{a}_1$, $\mathbf{a}_2$, $\cdots$, $\mathbf{a}_L$ is $\text{rank}(\mathbf{A})=L$ [27]. Since $\mathbf{d}_{\mathbf{s}^{(1)}}$, $\mathbf{d}_{\mathbf{s}^{(2)}}$, $\cdots$, $\mathbf{d}_{\mathbf{s}^{(G)}}$ are orthogonal to each other, they constitute basis of a G dimensional signal space, $\mathcal{G}$, i.e., $\text{rank}(\mathbf{G})=G$ where $\mathbf{G}=[\mathbf{d}_{\mathbf{s}^{(1)}}\ \cdots\ \mathbf{d}_{\mathbf{s}^{(g)}}\ \cdots\ \mathbf{d}_{\mathbf{s}^{(G)}}]$ and $\mathbf{d}_{\mathbf{s}^{(g)}}$ is a basis vector.

Since matrix $\mathcal{I}$ consists of D groups of effective interferences projected on the desired signals subspace $\mathcal{G}$, we have $\text{rank}(\mathcal{I})\leq\text{rank}(\mathbf{G})=G$. Then, according to Theorem 1, given D interference groups, CIA-PA is applicable under $\text{rank}(\mathcal{I})<D$. Therefore, when $D\geq G+1$, we can derive $\text{rank}(\mathcal{I})<D$ from $\text{rank}(\mathcal{I})\leq G$, yielding the feasibility of CIA-PA. So, Lemma 3 follows. ■

References

[1] N. Yang, L. Wang, G. Geraci, M. Elkashlan, J. Yuan, and M. Di Renzo, "Safeguarding 5G wireless communication networks using physical layer security," *IEEE Commun. Mag.*, vol. 53, no. 4, pp. 20–27, Apr. 2015.

[2] (2014). *Enterprise Mobility 4.1 Design Guide*. [Online]. Available: https://www.cisco.com/c/en/us/td/docs/solutions/Enterprise/Mobility/emob41dg/emob41dg-wrapper.html

[3] D. Tse and P. Viswanath, *Fundamentals of Wireless Communication*. New York, NY, USA: Cambridge Univ. Press, 2005.

[4] J. Chen, A. Singh, P. Elia, and R. Knopp, "Interference neutralization for separated multiuser uplink-downlink with distributed relays," in *Proc. Inf. Theory Appl. Workshop*, Feb. 2011, pp. 1–9.

[5] Z. Li, K. G. Shin, and L. Zhen, "When and how much to neutralize interference?" in *Proc. IEEE Conf. Comput. Commun. (IEEE INFOCOM)*, May 2017, pp. 1–9.

[6] Z. Li, Y. Liu, K. G. Shin, J. Liu, and Z. Yan, "Interference steering to manage interference in IoT," *IEEE Internet Things J.*, vol. 6, no. 6, pp. 10458–10471, Dec. 2019.

[7] Z. Li, Y. Liu, K. G. Shin, J. Li, F. Guo, and J. Liu, "Design and adaptation of multi-interference steering," *IEEE Trans. Wireless Commun.*, vol. 18, no. 7, pp. 3329–3346, Jul. 2019.

[8] Taesa and A. Goldsmith, "On the optimality of multiantenna broadcast scheduling using zero-forcing beamforming," *IEEE J. Sel. Areas Commun.*, vol. 24, no. 3, pp. 528–541, Mar. 2006.

[9] G. Bresler, D. Cartwright, and D. Tse, "Feasibility of interference alignment for the MIMO interference channel," *IEEE Trans. Inf. Theory*, vol. 60, no. 9, pp. 5573–5586, Sep. 2014.

[10] V. Ntranos, M. A. Maddah-Ali, and G. Caire, "Cellular interference alignment," *IEEE Trans. Inf. Theory*, vol. 61, no. 3, pp. 1194–1217, Mar. 2015.

[11] V. R. Cadambe and S. A. Jafar, "Interference alignment and degrees of freedom of the K-user interference channel," *IEEE Trans. Inf. Theory*, vol. 54, no. 8, pp. 3425–3441, Aug. 2008.

[12] M. A. Maddah-Ali, A. S. Motahari, and A. K. Khandani, "Communication over MIMO X channels: Interference alignment, decomposition, and performance analysis," *IEEE Trans. Inf. Theory*, vol. 54, no. 8, pp. 3457–3470, Aug. 2008.

[13] C. M. Yetis, T. Gou, S. A. Jafar, and A. H. Kayran, "On feasibility of interference alignment in MIMO interference networks," *IEEE Trans. Signal Process.*, vol. 58, no. 9, pp. 4771–4782, Sep. 2010.

[14] S. A. Jafar and S. Shamai (Shitz), "Degrees of freedom region of the MIMO X channel," *IEEE Trans. Inf. Theory*, vol. 54, no. 1, pp. 151–170, Jan. 2008.

[15] X. Bing, X. Xianzhong, M. Bin, and L. Weijia, "An optimized cooperative interference alignment algorithm for MIMO interference channel," in *Proc. Int. Conf. Comput. Sci. Netw. Technol.*, Dec. 2011, pp. 1063–1067.

[16] V. S. Annapureddy, A. El Gamal, and V. V. Veeravalli, "Degrees of freedom of interference channels with CoMP transmission and reception," *IEEE Trans. Inf. Theory*, vol. 58, no. 9, pp. 5740–5760, May 2012.

[17] H. Huang and V. K. N. Lau, "Partial interference alignment for K-user MIMO interference channels," *IEEE Trans. Sig. Process.*, vol. 59, no. 10, pp. 4900–4908, Oct. 2011.

[18] F. Pantisano, M. Bennis, W. Saad, and M. Debbah, "Cooperative interference alignment in femtocell networks," in *Proc. IEEE Global Telecommun. Conf. (GLOBECOM)*, Dec. 2011, pp. 1–6.

[19] Z. Li, J. Chen, L. Zhen, S. Cui, K. G. Shin, and J. Liu, "Coordinated multi-point transmissions based on interference alignment and neutralization," *IEEE Trans. Wireless Commun.*, vol. 18, no. 7, pp. 3347–3365, Jul. 2019.

[20] Z. Li, Y. Bai, J. Liu, J. Chen, and Z. Chang, "Adaptive proportional fair scheduling with global-fairness," *Wireless Netw.*, vol. 25, no. 8, pp. 5011–5025, Nov. 2019.

[21] E. Perahia and R. Stacey, *Next Generation Wireless LANs: 802.11n and 802.11ac*, 2nd ed. New York, NY, USA: Cambridge Univ. Press, 2013.

[22] *IEEE Standard for Information Technology–Telecommunications and Information Exchange Between Systems Local and Metropolitan Area Networks–Specific Requirements Part 11: Wireless LAN Medium Access Control (MAC) and Physical Layer (PHY) Specifications Amendment 3: Enhancements for Very High Throughput to Support Chinese Millimeter Wave Frequency Bands(60 GHz and 45 GHz)*, document 802.11 WG - Wireless LAN Working Group, IEEE 802.11aj-2018, 2018.

[23] S. Sen, R. Roy Choudhury, and S. Nelakuditi, "CSMA/CN: Carrier sense multiple access with collision notification," *IEEE/ACM Trans. Netw.*, vol. 20, no. 2, pp. 544–556, Apr. 2012.

[24] S. Rayanchu, A. Mishra, D. Agrawal, S. Saha, and S. Banerjee, "Diagnosing wireless packet losses in 802.11: Separating collision from weak signal," in *Proc. 27th Conf. Comput. Commun. (IEEE INFOCOM)*, Apr. 2008, pp. 1409–1417.

[25] (2020). *5G White Paper*. [Online]. Available: https://www.ngmn.org/work-programme/5g-white-paper.html

[26] Z. Li, J. Ding, X. Dai, K. G. Shin, and J. Liu, "Exploiting interactions among signals to decode interfering transmissions with fewer receiving antennas," *Comput. Commun.*, vol. 136, pp. 63–75, Feb. 2019.

[27] X. Zhang, *Matrix Analysis and Applications*. Beijing, China: Tsinghua Univ. Press, 2004.

Zhao Li (Member, IEEE) received the B.S. degree in telecommunications engineering and the M.S. and Ph.D. degrees in communication and information systems from Xidian University, Xi'an, China, in 2003, 2006, and 2010, respectively. He worked as a Visiting Scholar and then Research Scientist with the Real-Time Computing Laboratory, Department of Electrical Engineering and Computer Science, University of Michigan, from 2013 to 2015. He is currently an Associate Professor with the School of Cyber Engineering, Xidian University. He has published over 40 technical articles at premium international journals and conferences, such as IEEE Internet of Things Journal, IEEE Transactions on Wireless Communications (TWC), IEEE INFOCOM, IEEE Transactions on Vehicular Technology (TVT), *Computer Communications*, and *Wireless Networks*. His research interests include wireless communication, 5G communication systems, resource allocation, interference management, the IoT, and physical layer security.

Jun Li is currently pursuing the master's degree with the School of Cyber Engineering, Xidian University. Her research interests include wireless communication and physical layer security.

Yinghou Liu is currently pursuing the master's degree with the School of Telecommunications Engineering, Xidian University. His research interests include wireless communication, resource allocation, and interference management.

Xiujuan Liang is currently pursuing the master's degree with the School of Cyber Engineering, Xidian University. Her research interests include wireless communication and physical layer security.

Kang G. Shin (Life Fellow, IEEE) received the B.S. degree in electronics engineering from Seoul National University, Seoul, South Korea, in 1970, and the M.S. and Ph.D. degrees in electrical engineering from Cornell University, Ithaca, NY, USA, in 1976 and 1978, respectively. He is currently the Kevin and Nancy O'Connor Professor of Computer Science and the Founding Director of the Real-Time Computing Laboratory, Department of Electrical Engineering and Computer Science, University of Michigan, Ann Arbor, MI, USA. At Michigan, he has supervised the completion of 82 PhDs and also chaired the Computer Science and Engineering Division for three years starting in 1991. From 1978 to 1982, he was on the faculty of the Rensselaer Polytechnic Institute, Troy, NY, USA. He has authored/coauthored more than 900 technical articles (more than 330 of which are published in archival journals) and more than 30 patents or invention disclosures. His current research interests include QoS-sensitive computing and networks as well as on embedded real-time and cyber-physical systems. He is also a fellow of ACM. He received numerous institutional awards and best paper awards.

Zheng Yan (Senior Member, IEEE) received the B.Eng. degree in electrical engineering and the M.Eng. degree in computer science and engineering from Xi'an Jiaotong University, Xi'an, China, in 1994 and 1997, respectively, the M.Eng. degree in information security from the National University of Singapore, Singapore, in 2000, and the Lic.Sc. degree and the D.Sc. (Tech.) degree in electrical engineering from the Helsinki University of Technology, Helsinki, Finland, in 2005 and 2007, respectively. She is currently a Professor with Xidian University, Xi'an, and a Visiting Professor with Aalto University, Espoo, Finland. She authored more than 150 peer-reviewed publications and solely authored two books. She is the inventor and the co-inventor of over 50 patents and PCT patent applications. Her research interests include trust, security and privacy, social networking, cloud computing, networking systems, and data mining. She also serves as an Associate Editor of *Information Sciences*, *Information Fusion*, IEEE Internet of Things Journal, *Journal of Network and Computer Applications* (JNCA), and *Security and Communication Networks*. She is also a leading guest editor of many reputable journals, including *ACM Transactions on Multimedia Computing, Communications, and Applications* (ACM TOMM), *Future Generation Computer Systems* (FGCS), IEEE Systems Journal, and *Mobile Networks and Applications* (MONET). She has served as a steering, organization, and program committee member for over 70 international conferences.

Hui Li (Member, IEEE) received the B.Sc. degree from Fudan University in 1990 and the M.Sc. and Ph.D. degrees from Xidian University, China, in 1993 and 1998, respectively. In 2009, he was a Visiting Scholar with the Department of Electrical and Computer Engineering (ECE), University of Waterloo. Since 2005, he has been a Professor with the School of Telecommunications Engineering, Xidian University. His research interests include the areas of cryptography, security of cloud computing, wireless network security, and information theory. He has served as the TPC Co-Chair for ISPEC 2009 and IAS 2009, and the General Co-Chair for E-Forensic 2010, ProvSec 2011, and ISC 2011.